

# Unveiling the Vulnerability of Private Fine-Tuning in Split-Based Frameworks for Large Language Models: A Bidirectionally Enhanced Attack

Guanzhong Chen  
Harbin Institute of Technology,  
Shenzhen  
Shenzhen, China  
muxichenz@outlook.com

Zhengan Qin  
Zhejiang University  
Hangzhou, China  
leonine@zju.edu.cn

Mingxin Yang  
Huazhong University of Science and  
Technology  
Wuhan, China  
ymx@hust.edu.cn

Yajie Zhou  
Zhejiang University  
Hangzhou, China  
yajiezhou@zju.edu.cn

Tao Fan  
Hong Kong University of Science and  
Technology  
Hong Kong, China  
Webank  
Shenzhen, China  
tfanac@cse.ust.hk

Tianyu Du\*  
Zhejiang University  
Hangzhou, China  
zjradty@zju.edu.cn

Zenglin Xu\*  
Fudan University; Shanghai Academy  
of AI for Science  
Shanghai, China  
Pengcheng Lab  
Shenzhen, China  
zenglinxu@fudan.edu.cn

## ABSTRACT

Recent advancements in pre-trained large language models (LLMs) have significantly influenced various domains. Adapting these models for specific tasks often involves fine-tuning (FT) with private, domain-specific data. However, privacy concerns keep this data undisclosed, and the computational demands for deploying LLMs pose challenges for resource-limited data holders. This has sparked interest in split learning (SL), a Model-as-a-Service (MaaS) paradigm that divides LLMs into smaller segments for distributed training and deployment, transmitting only intermediate activations instead of raw data. SL has garnered substantial interest in both industry and academia as it aims to balance user data privacy, model ownership, and resource challenges in the private fine-tuning of LLMs. Despite its privacy claims, this paper reveals significant vulnerabilities arising from the combination of SL and LLM-FT: *the Not-too-far property of fine-tuning and the auto-regressive nature of LLMs*. Exploiting these vulnerabilities, we propose Bidirectional

Semi-white-box Reconstruction (BiSR), the first data reconstruction attack (DRA) designed to target both the forward and backward propagation processes of SL. BiSR utilizes pre-trained weights as prior knowledge, combining a learning-based attack with a bidirectional optimization-based approach for highly effective data reconstruction. Additionally, it incorporates a Noise-adaptive Mixture of Experts (NaMoE) model to enhance reconstruction performance under perturbation. We conducted systematic experiments on various mainstream LLMs and different setups, empirically demonstrating BiSR's state-of-the-art performance. Furthermore, we thoroughly examined three representative defense mechanisms, showcasing our method's capability to reconstruct private data even in the presence of these defenses.

## CCS CONCEPTS

• Security and privacy → Distributed systems security;

## KEYWORDS

Large Language Models, Split Learning, Data Reconstruction Attack

## ACM Reference Format:

Guanzhong Chen, Zhengan Qin, Mingxin Yang, Yajie Zhou, Tao Fan, Tianyu Du, and Zenglin Xu. 2024. Unveiling the Vulnerability of Private Fine-Tuning in Split-Based Frameworks for Large Language Models: A Bidirectionally Enhanced Attack. In *Proceedings of the 2024 ACM SIGSAC Conference on Computer and Communications Security (CCS '24)*, October 14–18, 2024, Salt Lake City, UT, USA. ACM, New York, NY, USA, 21 pages. <https://doi.org/10.1145/3658644.3690295>

\*Corresponding authors.

Permission to make digital or hard copies of all or part of this work for personal or classroom use is granted without fee provided that copies are not made or distributed for profit or commercial advantage and that copies bear this notice and the full citation on the first page. Copyrights for components of this work owned by others than the author(s) must be honored. Abstracting with credit is permitted. To copy otherwise, or republish, to post on servers or to redistribute to lists, requires prior specific permission and/or a fee. Request permissions from [permissions@acm.org](mailto:permissions@acm.org).

CCS '24, October 14–18, 2024, Salt Lake City, UT, USA

© 2024 Copyright held by the owner/author(s). Publication rights licensed to ACM.

ACM ISBN 979-8-4007-0636-3/24/10

<https://doi.org/10.1145/3658644.3690295>

## 1 INTRODUCTION

Large language models (LLMs), such as the GPT series [6, 31, 35, 36] and LLaMA [46, 47], have demonstrated exceptional performance across various domains. This success is largely due to the prevalent *pre-train then fine-tune* paradigm. In this approach, models are first pre-trained on extensive public domain datasets (spanning hundreds of gigabytes) to develop foundational capabilities, and then fine-tuned on smaller, task-specific datasets to adapt the model to particular domains. Given the substantial costs associated with the pre-training phase and the billions of parameters in LLMs, fine-tuning (FT) a pre-trained foundation model (particularly with parameter-efficient fine-tuning (PEFT)) stands out as the most cost-effective approach for real-world applications. However, despite the reduced costs of fine-tuning, most users still lack the computational resources and technical expertise to independently obtain and fine-tune LLMs. This has led to the emergence of a new business model known as Model-as-a-Service (MaaS). In MaaS, enterprises with sufficient computational resources and technical capabilities (referred to as model vendors) offer LLMs as cloud services, providing customers with fine-tuning APIs that allow them to customize LLMs using their own data.

While MaaS offers customers efficient and customizable LLM services, it also presents significant privacy risks. On one hand, transmitting raw customer data through FT APIs to model vendors can result in direct data leakage. On the other hand, sending the entire LLM to customers for local fine-tuning is impractical, as the large size of LLMs often exceeds customers' limited capacity, and the weights of LLMs are generally considered valuable proprietary assets by model vendors and cannot be disclosed. In this context, a distributed machine learning framework known as split learning (SL) [19, 49] has emerged as a promising solution that effectively balances data privacy with model privacy. SL involves partitioning and deploying models between the client-side (customer) and server-side (model vendor), enabling model vendors to utilize their extensive computational resources while keeping the majority of LLMs undisclosed. At the same time, users need only upload intermediate activations (referred to as *smashed data*) to avoid direct exposure of their sensitive data. Consequently, SL for LLMs has garnered substantial interest in both industry and academia [9, 40, 51].

However, prior research indicates that even with the use of intermediate data, adversaries can still execute privacy attacks, such as property inference attacks [29], membership inference attacks [38, 41], and data reconstruction attacks [22, 32, 34, 54]. Among these, the data reconstruction attack (DRA) is of particular concern, as it constitutes the most severe breach of user privacy by attempting to reconstruct the user's original data. While DRAs have been extensively studied in traditional SL with discriminative models and standard classification tasks, there is a notable absence of research on SL involving LLMs in the existing literature. This paper seeks to address the question: *Are generative LLMs in SL also susceptible to DRAs?*

Different from conventional SL, integrating LLMs into SL introduces two notable features: (i) *Reliance on Pre-trained Weights*: Traditional SL typically involves simple model architectures with small-scale parameters, where client models are often initialized

with random parameters and trained from scratch [2, 43, 48]. In contrast, LLM-based approaches utilize pre-trained weights, which provide essential language modeling capabilities crucial for effective FT. Consequently, existing frameworks [9, 40] either require clients to access publicly available LLM weights or distribute portions of pre-trained LLMs directly to clients, allowing client-side models to inherit these pre-trained weights. (ii) *Generation Task*: Whereas conventional SL primarily focuses on discriminative models and classification tasks, mainstream LLMs are typically causal language modeling (CLM) models designed for natural language generation (NLG) tasks.

**Our work.** Focusing on the scenario involving an *honest-but-curious server* as the adversary, we extend earlier findings and argue that the two new features introduced by the combination of SL and LLM FT lead to even higher privacy threats from DRAs. We identify *two vulnerabilities* that contribute to this amplification but are not captured by existing DRAs.

**Vulnerability<sub>1</sub> – The "Not-too-far" Property of LLM FT.** The FT process's reliance on pre-trained weights provides adversaries with significant prior knowledge, due to a critical characteristic observed during LLM FT: the "Not-too-far" property. This property suggests that the features embedded in the pre-trained weights, which are crucial for DRAs, remain largely *unchanged* during FT. Consequently, even if the client's model weights diverge from the pre-trained state, attackers can still leverage the pre-trained weights to conduct straightforward yet highly effective DRAs.

**Vulnerability<sub>2</sub> – The Auto-regressive Nature of LLMs.** Mainstream LLMs are CLM models that predict the next token based on the preceding sequence. During training, these models exhibit auto-regressive behavior, generating training labels by shifting the input sequence left by one token (teacher-forcing). This creates an overlap in the solution space for reconstructing both the label and the input. Such alignment enables adversaries to exploit both forward smashed data and backward gradients for *bidirectional* attacks. Moreover, in the SL setting, the known-forward-activation trait eliminates the sequence order issue in gradient-based DRAs for language models, allowing adversaries to achieve greater reconstruction accuracy.

To fully exploit these vulnerabilities, we propose a novel DRA method called **Bidirectional Semi-white-box Reconstruction (BiSR)**, the first DRA paradigm specifically targeting LLMs fine-tuned within the SL framework. BiSR integrates a learning-based reconstruction, which trains an inversion model to recover the original input from the smashed data, and an optimization-based reconstruction, which approximates the raw input through iterative optimization. To leverage Vulnerability<sub>1</sub>, BiSR employs pre-trained weights as an attack prior via *semi-white-box access* (defined in Section 2.4) for both the learning-based and optimization-based reconstruction processes. To exploit Vulnerability<sub>2</sub>, the optimization-based stage of BiSR capitalizes on the overlap in the solution space, leveraging both forward (smashed data) and backward (gradient) information to conduct a highly effective *bidirectional* attack.

**Contributions.** To the best of our knowledge, this work represents the first study on DRAs within the SL framework for LLM fine-tuning. Our contributions can be summarized as the following:

- **New insights.** We present the insight that the combination of SL and LLMs brings about two new crucial vulnerabilities that greatly amplify the threat of DRAs and are not captured by existing DRA methods: the "Not-too-far" property of LLM-FT and the auto-regressive nature of LLMs.
- **Novel Approach.** We introduce Bidirectional Semi-white-box Reconstruction (BiSR), the first DRA that integrates learning-based and optimization-based methods to bidirectionally attack both forward and backward transmissions in SL. Additionally, we propose the Noise-adaptive Mixture of Experts (NaMoE) inversion model to enhance its perturbation adaptability.
- **Systematic Experiments.** We conduct thorough experiments to evaluate various DRAs across different mainstream LLMs and FT datasets under a range of conditions. We also assess their attack performance against three types of defense mechanisms. Our results reveal the effectiveness and superiority of BiSR compared to baseline methods and its adaptability to perturbation-based defenses, highlighting the significant privacy risks associated with split-based LLM fine-tuning frameworks.
- Our code is available at GitHub repository <https://github.com/StupidTrees/SplitLLM>.

## 2 PRELIMINARIES

### 2.1 Fine-Tuning of LLMs

The "pre-train then fine-tune" approach is widely used for training LLMs and adapting them for practical applications. In contrast to the data-intensive and computationally demanding pre-training phase, the fine-tuning (FT) process requires smaller datasets and fewer computational resources but is essential for real-world deployment of LLMs.

Current FT of LLMs primarily focuses on supervised fine-tuning (SFT) for NLG tasks, where the target sentence to be generated serves as the label for supervised training. Unlike encoder-only models such as BERT [13], which are better suited for classification tasks due to their masked language modeling (MLM) characteristics, encoder-decoder models like T5 [37] and decoder-only models like GPT [6, 35, 36] and LLaMA [46, 47] are extensively used in NLG tasks due to their causal language modeling (CLM) properties, where the modeling of each token is based solely on its preceding tokens. These models typically comprise an auto-regressive decoder structure.

During the SFT of CLM models, the *teacher forcing* [52] strategy is employed. In this approach, the tokens preceding a target token in a sentence serve as inputs to train the decoder to predict that token. Let  $w_t$  represent the token at position  $t$ , and  $\hat{y}_t[w]$  denote the model's predicted probability for the next token  $w$  at that position, i.e., the prediction for position  $t + 1$ . The loss for each time step during the teacher forcing phase is defined as:

$$\mathcal{L}_{CE}(\hat{y}_t, y_t) = -\log \hat{y}_t[w_{t+1}], \quad (1)$$

which corresponds to the negative log probability of the model's prediction for the true token at the next position. Consequently, for each sentence  $x$  of length  $T$  in the SFT dataset, with the model

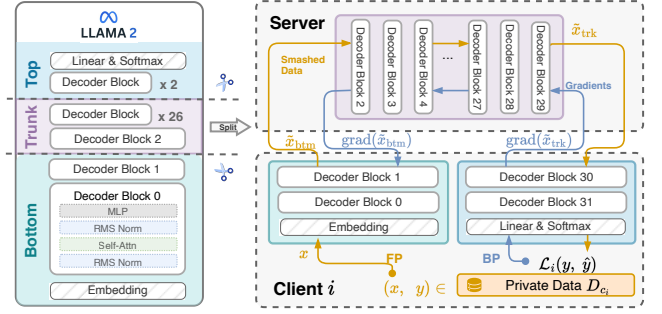


**Figure 1: The private-label SL framework for fine-tuning LLaMA2-chat-7B, illustrated with a single client. The model's 32 decoder blocks are divided into three segments: *Bottom* (embedding layer and the first two blocks), *Trunk* (middle 28 blocks), and *Top* (final two blocks, normalization layer, and linear layer). The client hosts the Bottom and Top segments, while the server manages the Trunk.**

output denoted as  $y = (y_1, y_2, \dots, y_T)$ , the training loss is:

$$\mathcal{L}_{LM} = \text{CrossEntropy}(y_{1:T-1}, x_{2:T}), \quad (2)$$

indicating that *the fine-tuning label is obtained by shifting the input sentence to the left by one token*. This type of loss is also referred to as the *auto-regressive target*.

### 2.2 Split Learning

The split learning (SL) architecture typically involves multiple clients  $c_1, c_2, \dots, c_n$  with private data  $D_{c_1}, D_{c_2}, \dots, D_{c_n}$  and a central server  $S$  that coordinates the learning process.

To collaboratively train a model  $f_{\theta}$  using private data  $D_{c_i}$  across clients, the model is partitioned. Common SL frameworks adopt two architectures [32]: (i) the non-private-label architecture, where clients share labels with the server and the model is divided into two segments, one held by the client and the other by the server, and (ii) the private-label architecture, where labels remain local and the model is divided into three segments, with the first and last segments residing on the client. We focus on the private-label architecture due to its enhanced privacy and the inherent non-disclosure of labels in LLM-FT scenarios, as depicted in Figure 1. The model  $f_{\theta}$  is split into three parts: the *Bottom*  $f_{\text{btm}}$  (input end), the *Trunk*  $f_{\text{trk}}$  (middle layers), and the *Top*  $f_{\text{top}}$  (output end), with the *cut-layers* being the final layers of each segment. The server hosts the parameter-intensive Trunk, while each client holds the lightweight Bottom and Top segments.

Model training in SL employs distributed forward and backward propagation [19]. Each step begins with a client encoding a batch  $x \in D_{c_i}$  through the model's Bottom part, generating intermediate activation  $\tilde{x}_{\text{btm}} = f_{\text{btm}}(x)$ , or *smashed data*, which is sent to the server. The server forwards  $\tilde{x}_{\text{btm}}$  through the Trunk, creating  $\tilde{x}_{\text{trk}} = f_{\text{trk}}(\tilde{x}_{\text{btm}})$ , and returns it to the client. The client then finalizes the forward pass through the Top part, yielding output  $\hat{y} = f_{\text{top}}(\tilde{x}_{\text{trk}})$ . Following loss computation  $\mathcal{L}_i(\hat{y}, y)$  using the private label  $y$ , backward propagation begins, with gradients flowing through Top-Trunk-Bottom, facilitated by intermediate gradients  $\text{grad}(\tilde{x}_{\text{trk}})$  and  $\text{grad}(\tilde{x}_{\text{btm}})$  exchanged between client and server.

In a standard scenario, it has been shown that the single-step SL process aligns with the centralized forward and backward passes for a client-server pair [19]. In the case of multiple clients, the traditional SL paradigm can be applied by sequentially training each client and then passing the parameters to the next [49]. Alternatively, synergistic methods that combine SL and federated learning (FL) can be utilized, allowing clients to participate concurrently in split learning with the server, which subsequently aggregates the gradients or model parameters [25, 43, 55]. However, the complex processing associated with multiple clients in SL is not directly relevant to the privacy data leakage issues addressed in this paper. Therefore, for clarity, we will limit our focus to a scenario involving a *single client*.

After completing SL, the model is partitioned between the server and the clients. During inference, a client executes the distributed forward process of SL on the input data. In auto-regressive NLG, the client feeds the prompt into the lower layers of the model, performs split forward propagation to generate the next token at the Top, appends this token to the partially generated sentence, and repeats the distributed process until the end-of-sentence token is produced.

### 2.3 Perturbation-based Privacy Protection methods for Split Learning

With the feasibility of SL validated by numerous studies, it has become standard practice to augment SL with additional privacy safeguards. In scenarios involving a curious server, perturbation-based non-cryptographic methods are commonly utilized. These primarily include approaches based on differential privacy (DP)[1], which add noise directly to the intermediate data[7, 17, 40, 45, 53], and NoPeek [50], which constrains intermediate representations through regularization terms.

**Embedding  $d_{\mathcal{X}}$ -Privacy** ( $d_{\mathcal{X}P}$ )[7] is a perturbation strategy specifically designed for language models within the SL framework. It perturbs the embedding space to satisfy  $d_{\mathcal{X}}$ -Privacy ( $d_{\mathcal{X}P}$ ), a relaxed version of Local DP[17]. Specifically, noise  $N$  is added to the output of the embedding layer  $\phi_x = \phi(x)$  as follows:

$$\phi'_x = \phi_x + N, ; p(N)(z) \propto \exp(-\epsilon|z|), \quad (3)$$

where  $\epsilon$  is the privacy parameter. Next, within the embedding space, the input embedding closest to the perturbed embedding is identified and used to replace the original embedding:

$$\phi_x = \underset{\phi \in \Phi}{\operatorname{argmin}} |\phi - \phi'_x|. \quad (4)$$

**Smashed-data DP** techniques, such as DP-Forward [15], add noise directly to the transmitted smashed data  $\tilde{x}$  and are widely used in SL systems [15, 45, 53]. Using the Laplace mechanism as an example, the smashed data is first clipped as follows:  $\tilde{x} \leftarrow \tilde{x}/\max(1, \frac{|x|}{G})$ , and then augmented with Laplace noise of a specified scale:

$$\tilde{x} \leftarrow \tilde{x} + \operatorname{Lap}(0, \frac{\Delta f_{\text{btm}}}{\epsilon}), \quad (5)$$

where  $G$  is the clipping threshold,  $\operatorname{Lap}(0, \sigma)$  denotes noise following the Laplace distribution with scale  $\sigma$ ,  $\epsilon$  is the differential privacy budget, and  $\Delta f_{\text{btm}}$  represents the sensitivity of the query function (i.e., the model segment  $f_{\text{btm}}$  that generates  $\tilde{x}$ ) with respect to the original data  $x$ .

**NoPeek-based perturbation** methods introduce a regularization term into the model's loss function to constrain the correlation between the intermediate smashed data  $\tilde{x}$  and the original input  $x$ , with the goal of minimizing the leakage of original information through the smashed data. The training loss for the model can be expressed as:

$$\mathcal{L}_{\text{nopeek}} = \mathcal{L}(\hat{y}, y) + \alpha \text{DCOR}(x, \tilde{x}), \quad (6)$$

where  $\alpha$  is a scalar weight that adjusts the strength of the regularization, and  $\text{DCOR}(x, \tilde{x})$  is a measure of distance correlation [50]. By incorporating this regularization term, NoPeek encourages the model segment prior to the cut layer (e.g.,  $f_{\text{btm}}$ ) to adapt such that the smashed data is as dissimilar from the original input as possible, effectively introducing a form of perturbation at the input level.

### 2.4 Threat Model

**Adversary's abilities.** We consider an *honest-but-curious* [33] server as the adversary. The "honest" aspect indicates that the adversary adheres to the SL protocol, thereby not compromising the efficiency of distributed learning (a particularly realistic assumption for the resource-intensive LLM training scenario). The "curious" aspect implies that the adversary seeks to access and potentially exploit intermediate data within the system to reconstruct the original private input. We attribute the following capabilities to a curious server: (i) Access to all clients' smashed data  $\tilde{x}_{\text{btm}}$  and the gradients  $\operatorname{grad}(\tilde{x}_{\text{trk}})$  during the FT process, (ii) White-box access to the model's Trunk part, (iii) *Semi-white-box access* to the model's Bottom and Top parts (on the client), and (iv) Access to an auxiliary dataset  $D_a$ , which may (but does not necessarily) resemble the client's private dataset  $D_{c_i}$ . We define semi-white-box access as follows:

**Definition: Semi-White-Box Access.** During an attack on an LLM undergoing FT, the adversary does not have access to the model's exact weights at any training step but is aware of the model's architecture and its pre-trained weights.

The *semi-white-box* access level lies between white-box and black-box scenarios. In the context of LLM-SL, the semi-white-box assumption is both realistic and reasonable. While the server does not have precise knowledge of the client's updated weights during SL, the pre-trained weights of LLMs are often publicly available or retained by the server as the model vendor. This prior knowledge about the client's model segments can be leveraged when launching attacks. As a result, adversaries can design attack strategies that closely resemble those in a white-box setting, but they must contend with a *fine-tuning gap*—the discrepancy between the pre-trained model and the fine-tuned model.

**Adversary's objective.** In the split-based FT process, the adversarial server performing DRA aims to *reconstruct* as many original texts  $(x, y) \in D_{c_i}$  from the client's private fine-tuning dataset  $D_{c_i}$  as possible.

## 3 THE PROPOSED BiSR METHOD

In this section, we introduce our DRA method targeting LLM fine-tuned with SL, Bidirectional Semi-white-box Reconstruction (BiSR), depicted in Figure 2. We begin by establishing the foundational

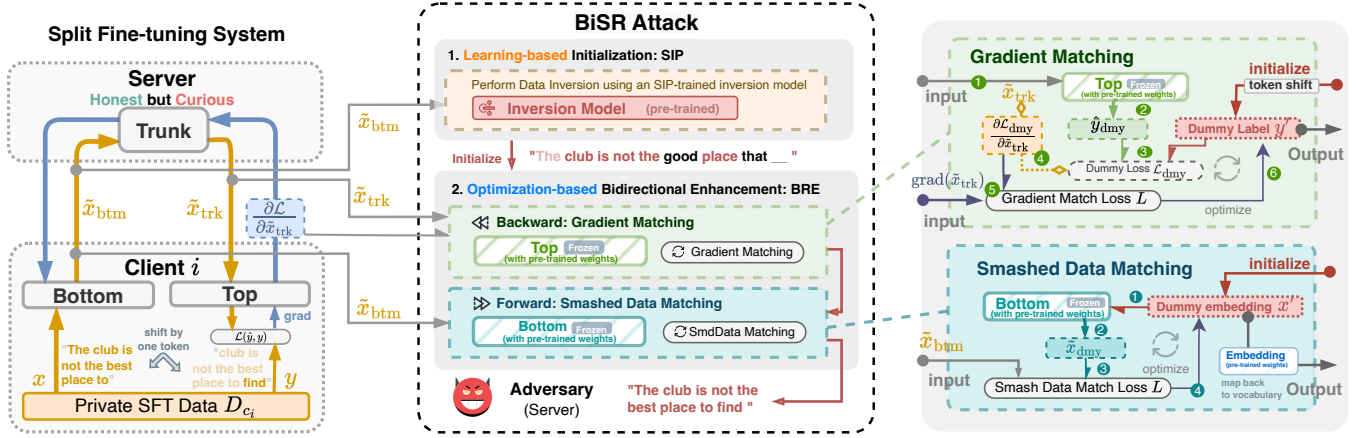


**Figure 2: The BiSR attack framework (middle) targeting the split-LLM-FT system (left). This two-stage attack starts with a learning-based approach, where the Semi-white-box Forward Inversion Paradigm (SIP)-trained attack model (NaMoE model) performs direct inversion on smashed data. The second stage builds upon the sentences initially recovered, employing both forward (using smashed data) and backward (using gradients) data for bidirectional, optimization-based enhancement. This process, detailed on the right, results in significantly more comprehensive sentence recovery.**

assumption underpinning BiSR for conducting semi-white-box attacks using pre-trained model priors.

**ASSUMPTION 1. Not-too-far:** *The fine-tuning of LLMs does not drastically alter the core characteristics established during the pre-training phase, which are adequate for both learning-based and optimization-based DRAs.*

This assumption posits that the intrinsic language modeling capabilities of LLMs, developed during pre-training, remain stable throughout the fine-tuning process for downstream tasks. Consequently, a fine-tuned LLM can generate intermediate outputs similar to those produced in its original, untuned state, thereby making semi-white-box access closely resemble white-box access. It is important to note that regardless of how clients personalize their model components (e.g., deviating in parameters or structure from pre-trained parts), as long as the intermediate results they produce (smashed data, gradients) are compatible with the pre-trained Trunk part on the server, they fall within the scope of the Not-too-far assumption. We empirically demonstrate that the Not-too-far assumption holds for LLMs in practice, even when clients adopt model components that are structurally or parametrically inconsistent with the pre-trained parts. Additionally, in Appendix F, we highlight through a comparison with image models that this assumption may be unique to language models.

Based on this assumption (utilizing Vulnerability<sub>1</sub>) and within the semi-white-box setting, BiSR implements a two-stage attack strategy, as depicted in Figure 2. The first stage employs Semi-white-box Forward Inversion Paradigm (SIP), a learning-based approach that trains an inversion model to recover input sentences from the smashed data, as detailed in subsection 3.1. Following this initial sentence recovery, a second-stage attack is initiated using Bidirectional Reconstruction Enhancement (BRE). This stage leverages Vulnerability<sub>2</sub> by utilizing both forward (smashed data) and backward (gradients) information for bidirectional optimization-based refinement, aiming to enhance reconstruction across various

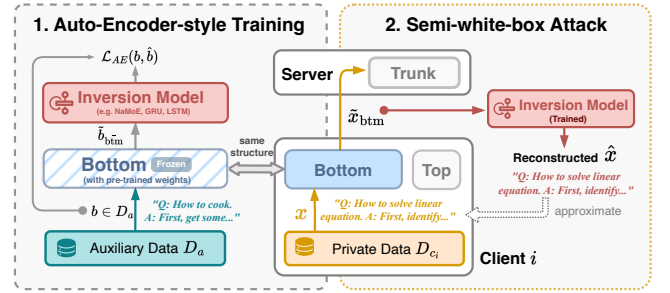


**Figure 3: The proposed Semi-white-box Forward Inversion Paradigm (SIP). During the training phase (left), the encoder mimicking the target model’s Bottom segment but with pre-trained parameters is frozen, while the decoder is trained on a dataset  $D_a$  similar to  $D_{c_i}$ , with original inputs  $b \in D_a$  as labels. In the attack stage (right), the inversion model receives the real model’s Bottom output  $\hat{x}_{btm}$ , the smashed data, and directly decodes it to obtain the attack results  $\hat{x}$ .**

domain datasets, as discussed in subsection 3.2. Additionally, to strengthen the resilience of the SIP-trained attack model against perturbation-based defense mechanisms, we introduce Noise-adaptive Mixture of Experts (NaMoE), an advanced inversion model for learning-based attacks, which is described in subsection 3.3.

### 3.1 Learning-based Initialization: SIP

Considering Vulnerability<sub>1</sub>, the first stage of BiSR involves a learning-based attack using an inversion model on smashed data. This model, trained on auxiliary data  $D_a$ , is designed to reconstruct the original data from the intermediate outputs of the LLM. The training and attack process of SIP is illustrated in Figure 3.

Viewing the Bottom part of the LLM as an encoder, SIP aims to train a malicious inversion model as a decoder, thereby forming

an auto-encoder system. We design an encoder  $e$  (mimicking the attacked LLM's Bottom segment) and a decoder  $d$  to be trained on an auxiliary dataset  $D_a$ , which may or may not be similar to the attacked data  $D_{c_i}$ . Our objective is to minimize the auto-encoder loss  $\mathbb{E}_{x \sim D_a} [\mathcal{L}_{AE}(d(e(x)), x)]$ , enabling  $d$  to function as the inversion model. For  $e$ , we select a model structurally identical to the Bottom segment of the attacked model but with *pre-trained weights* (i.e., semi-white-box access to the client's Bottom model), referred to as  $f_{\tilde{b}_{\text{btm}}}$ , to replicate  $f_{\text{btm}}$ . During the auto-encoder-style training, we freeze  $e$  and train only the decoder.

Assuming the target LLM has a vocabulary size of  $V$  and a hidden size of  $H$ , each batch of text (represented as token IDs with a unified sequence length  $S$ ) from the auxiliary dataset  $b^{B \times S \times 1} \in D_a$  is encoded by  $e = f_{\tilde{b}_{\text{btm}}}$ , resulting in  $f_{\tilde{b}_{\text{btm}}}(b) = \tilde{b}_{\text{btm}}^{B \times S \times H}$ . The decoder  $d$  (which could be a linear model, RNN, etc.) then decodes  $\tilde{b}_{\text{btm}}$  to produce  $d(\tilde{b}_{\text{btm}}) = \hat{b}^{B \times S \times V}$ . We use cross-entropy as the auto-encoder loss, defined as  $\mathcal{L}_{AE}(\hat{b}, b) = \text{CrossEntropy}(\hat{b}, b)$ . After training, the adversary conducts an attack by decoding the observed smashed data  $\tilde{x}_{\text{btm}}$  using the decoder  $d$  to recover  $\tilde{x} = d(\tilde{x}_{\text{btm}})$ , which approximates the original private data  $x$ .

The effectiveness of the auto-encoder-trained inversion model is anticipated to rely on Assumption 1, the degree of similarity between  $D_a$  and the target dataset  $D_{c_i}$ , and the precise alignment of the encoder  $e = f_{\tilde{b}_{\text{btm}}}$  with the Bottom segment of the target LLM. In Section 4.2, we will validate Assumption 1 and demonstrate that the inversion model trained using SIP exhibits *strong versatility*, attributed to its capacity for dual learning of both structural and semantic information. This model proves effective in cross-dataset scenarios (training SIP on one dataset while attacking SL on another with a different data distribution) and cross-layer scenarios (training DRA with  $e$  having a different number of layers than the emulated segment). Moreover, it demonstrates robustness to discrepancies between the weights of  $e$  and the emulated segment and shows potential adaptability to forward noise addition.

In practice, adversaries can apply the SIP-trained inversion model to smashed data from various layers of the LLM. This process produces a substantially reconstructed version of the original input, serving as a strong initialization point for the optimization-based DRA process discussed in the following section. Such initialization effectively mitigates the local optima issue in non-convex optimization [26], thereby significantly enhancing the final accuracy, as illustrated in Figure 4.

### 3.2 Optimization-based Enhancement: BRE

The SIP-trained inverter can initially generate high-quality data reconstructions, but it still faces performance bottlenecks due to the *fine-tuning gap* in semi-white-box assumption and the disparity between  $D_a$  and real data. To overcome these challenges, BiSR progresses from initial reconstruction to a second stage, leveraging both vulnerability<sub>1</sub> and vulnerability<sub>2</sub>. It employs an *optimization-based* approach, Bidirectional Reconstruction Enhancement (BRE), which attacks in *two directions* to utilize the *posterior information* observed during the SL process to mitigate the *fine-tuning gap* for higher-precision reconstruction.

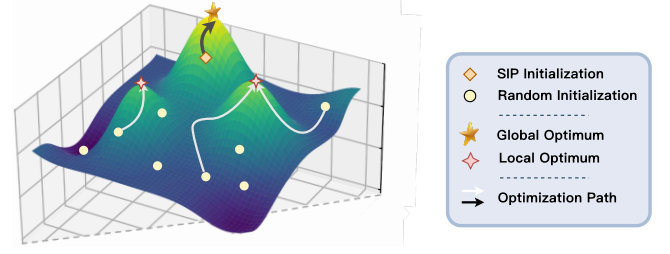


**Figure 4: Demonstration of the impact of BiSR's learning-based initialization (SIP) on optimization-based process: providing an effective starting point for achieving global optima.**

**3.2.1 Forward Enhancement by Smashed-Data Matching.** In the forward direction, existing DRAs assume white-box access, utilizing the smashed data  $\tilde{x}_{\text{btm}}$  to perform relaxed optimization in a discrete vocabulary space for attacks [42]. However, in SL, the adversary lacks white-box access, and within the LLM context, relaxed optimization becomes increasingly challenging and unstable due to the larger vocabulary space and model parameters (see Section 4). To address these challenges, BiSR shifts to continuous optimization in the embedding space under a semi-white-box setting.

Specifically, we construct a dummy embedding  $e'$  and iteratively optimize it to make the model's output smashed data  $\tilde{x}'_{\text{btm}}$  approximate the observed  $\tilde{x}_{\text{btm}}$ , expecting  $e'$  to approach the real embedding. Unlike previous work, the adversary has only semi-white-box access to the Bottom part of the model, meaning they can access  $f_{\tilde{b}_{\text{btm}}}$  but not  $f_{\text{btm}}$ . The optimization process is as follows:

$$e^* = \underset{e'}{\operatorname{argmin}} \mathcal{D}(f'_{\tilde{b}_{\text{btm}}}(e'), \tilde{x}_{\text{btm}}), \quad (7)$$

where  $\mathcal{D}$  is a distance function. Unlike [42], we use cosine similarity rather than Euclidean distance as the loss function. This method effectively addresses the challenges associated with high-dimensional embeddings in LLMs (details in Appendix D.5), leading to significantly improved empirical reconstruction performance.

After optimization, using the embedding layer  $\text{emb}()$  of the pre-trained model, we can identify the sentence  $x^*$  in the vocabulary space whose embedding is closest to  $e^*$ , which is then output as the reconstruction result:

$$x^* = \underset{x'}{\operatorname{argmin}} \|\text{emb}(x') - e^*\|. \quad (8)$$

In reverse, to initiate this optimization process with a previously reconstructed text, we simply pass the sentence through  $\text{emb}()$  to obtain its embedding, then proceed directly with optimization.

**3.2.2 Backward Enhancement by Gradient Matching.** The combination of SL and LLM fine-tuning enables the reconstruction of original data *in the backward direction* (Vulnerability<sub>2</sub>). To achieve this, BRE employs a gradient matching attack (GMA)-based approach. Previous GMAs [3, 12, 57] have primarily targeted FL systems, framing the attack as an optimization problem. Specifically, for a network  $f_\theta$  and a loss function  $\mathcal{L}$ , given a private training sample  $x$  with label  $y$ , an attacker with white-box access to  $f_\theta$  and the true gradient  $\nabla_\theta \mathcal{L}_\theta(x, y)$  can generate a randomly initialized dummy sample  $(x', y')$ , compute a dummy gradient through  $f_\theta$ ,

and optimize the gradient-matching loss [57] to minimize the discrepancy between the true gradient  $\nabla_{\theta} \mathcal{L}_{\theta}(x, y)$  and the dummy gradient  $\nabla_{\theta} \mathcal{L}_{\theta}(x', y')$ , thereby making  $x'$  and  $y'$  approximate the original private data.

BRE adapts GMA to the private-label SL scenario, where  $f_{\theta}$  corresponds to the model's Top segment  $f_{\text{top}}$ , and the input  $x$  becomes  $\tilde{x}_{\text{trk}}$ . The adversary has only semi-white-box access to  $f_{\theta}$ , meaning they can only access the mimic network  $f_{\text{top}}$ . After completing forward propagation, the client sends the gradient  $\text{grad}(\tilde{x}_{\text{trk}}) = \nabla_{\tilde{x}_{\text{trk}}} \mathcal{L}_{\text{top}}(\tilde{x}_{\text{trk}}, y)$  to the curious server, enabling a GMA. This process includes generating a dummy ground truth  $y'$  (which must be a probability distribution over the vocabulary), passing  $\tilde{x}_{\text{trk}}$  through the mimic network  $f_{\text{top}}$ , calculating the dummy loss  $\mathcal{L}_{\text{dmy}}(\tilde{x}_{\text{trk}}, y')$ , and minimizing the discrepancy between the gradient of the dummy loss and the real gradient represented by:

$$L(y') = \beta \|\nabla_{\tilde{x}_{\text{trk}}} \mathcal{L}_{\text{dmy}}(\tilde{x}_{\text{trk}}, y') - \nabla_{\tilde{x}_{\text{trk}}} \mathcal{L}(\tilde{x}_{\text{trk}}, y)\|_2 + (1 - \beta) \|\nabla_{\tilde{x}_{\text{trk}}} \mathcal{L}_{\text{dmy}}(\tilde{x}_{\text{trk}}, y') - \nabla_{\tilde{x}_{\text{trk}}} \mathcal{L}(\tilde{x}_{\text{trk}}, y)\|_1, \quad (9)$$

where a combined distance of L2 norm and L1 norm is adopted, similar to TAG [12], to enhance the attack performance on language models, with  $\beta$  serving as a coefficient parameter. It is important to note that GMAs in FL settings often encounter the *sequence order issue*, where the reconstructed input  $x'$  may be token-wise permuted. However, CLM's input-label alignment (detailed later) and SL's known-forward-activation trait eliminate this issue, allowing adversaries to obtain a correctly ordered sequence by simply optimizing  $y'$ .

What makes GMA effective for input-data reconstruction in SL is LLM's *auto-regressive FT objective*, which ensures alignment between the reconstruction of label and the input. Specifically, the  $y$  to be recovered is a left-shifted version of the original input  $x$ , corresponding to  $\tilde{x}_{\text{trk}}$ . This alignment enables the *collaborative use* of BRE's forward and backward reconstruction processes, thereby significantly enhancing attack performance.

In practice, the forward and backward enhancements of BRE can be utilized in two ways: (1) sequentially, where gradient matching is performed first, followed by smashed-data matching. For the output  $\hat{x}_{\text{SIP}}^{B \times T \times V}$  of SIP, softmax is applied along its last dimension to initialize dummy labels  $y'$  for gradient matching, then after several rounds of gradient matching, the resulting  $\hat{x}_{\text{GM}}$  is processed with a pre-trained embedding layer to obtain initial  $e'$  for smashed-data matching, resulting in  $\hat{x}_{\text{SM}}$ . This method is denoted as BiSR (b+f) in the experimental section. (2) Independently, where gradient matching and smashed-data matching are performed separately on the results of SIP. This is denoted as BiSR (b) and BiSR (f) in the experimental section, respectively. Adversaries can modularly employ BiSR to adapt to different scenarios of forward and backward perturbations.

### 3.3 Adapting to Noise: NaMoE Model

Another goal of BiSR is to provide adaptability against privacy-preserving methods that perturb intermediate outputs in the *forward* direction. In the curious server scenario, perturbation serves as the primary non-cryptographic technique for privatizing SL's smashed data. Methods include adding noise directly to the smashed

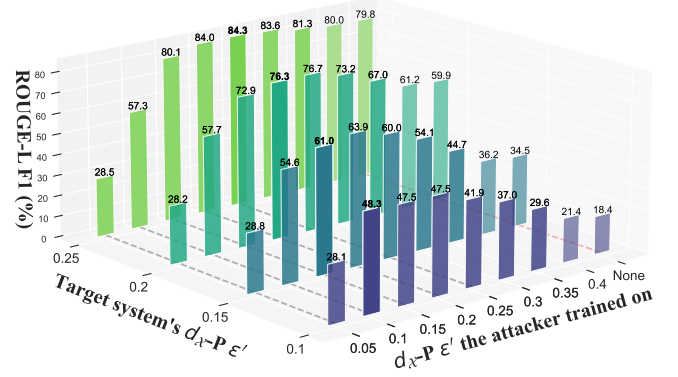


Figure 5: Performance boost brought by noise-aware training, demonstrated by attack performance (ROUGE-L F1 Score %) of inverters trained with embedding- $d_{X-P}$ -awareness on split-FT systems using embedding-glsdpx with varying noise scales, evaluated on GPT2-large and PIQA datasets.

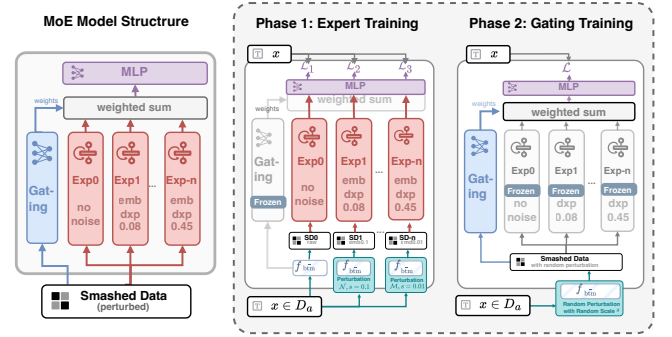


Figure 6: Proposed NaMoE model structure (left) and its training process (right). Each "Exp" represents an Expert handling a specific noise scale under a particular perturbation mechanism. The "emb" denotes Embedding- $d_{X-P}$ .

data [45, 53] or to the output of the embedding layer [17, 40]. These techniques not only degrade the performance of DRA, particularly optimization-based DRA, but also negatively impact model training performance, requiring more iterations to converge. Nevertheless, the ability of models to converge despite noise demonstrates their adaptability to forward perturbations under supervision.

This raises an intriguing question: *Can learning-based inversion models also adapt to forward perturbations similar to LLMs?* To explore this, we first highlight the similarity between the split-FT system (Bottom-Trunk-Top) and SIP's training system (Bottom-inversion model): (1) Both systems share a Bottom LLM segment with weights that are *Not-too-far* from the pre-trained state. (2) They follow similar training paradigms, with the former's FT label being the input sentence shifted by one token, while the latter's training label is the original input sentence.

Consequently, when perturbations impact the forward path, the noise in the smashed data necessitates adjustments in the SL system's Trunk and Top layers via the FT label to correct these disturbances and maintain functionality. Similarly, if noise is introduced

during SIP’s training phase (*noise-aware training*), the inversion model should be guided by the auto-encoder training label to develop perturbation correction capabilities. This leads us to the following observation:

**Observation:** *Noise-aware-trained inversion models adapt more effectively to perturbations and achieve superior attack performance compared to their noise-unaware counterparts.*

More specifically, consider a model  $f$  with a perturbation strategy (noise scale  $s$ ) represented as  $\mathcal{N}_s(f)$ . If an adversary knows the perturbation strategy  $\mathcal{N}$  used by the target and uses  $e = \mathcal{N}_{s'}(f_{\text{bim}})$  instead of  $e = f_{\text{bim}}$  during SIP’s auto-encoder-style training phase, the noise-aware trained inversion model can significantly improve performance when attacking an SL system using the same perturbation strategy  $\mathcal{N}_s$ . Furthermore, the closer the noise scale  $s'$  used by the attacker is to the real noise scale  $s$ , the higher the attack accuracy, as illustrated in Figure 5.

Building on this observation, a straightforward attack enhancement strategy could involve the adversary pre-training multiple DRA models on various noise scales and then deploying these models concurrently during the attack phase, choosing the highest-quality attack outcomes (evaluated by perplexity, for instance). However, this approach has the significant limitation that the adversary must anticipate the target’s potential noise scales in advance and can only select from a restricted set of candidates with uncertain quality. To address this limitation, this paper introduces the Noise-adaptive Mixture of Experts (NaMoE) model, which incorporates the adaptability of different expert models to various noise scales. This enables adversaries to conduct DRA effectively even without knowledge of the target’s specific privacy strategies.

As depicted in Fig. 6 (left), the NaMoE model primarily comprises several expert networks and a gating network. Each expert network simultaneously decodes smashed data inputs, with the results weighted and combined based on the gating network’s weights and processed by the output layer to yield the final attack outcome.

The NaMoE model utilizes a two-stage training approach, illustrated in Fig. 6 (right). In the first stage, with the gating network frozen, each attack dataset sample  $x \in D_a$  undergoes forward propagation with noise added per the perturbation mechanism  $\mathcal{N}$  and noise scale  $s'$  for each expert, creating personalized smashed data  $\tilde{x} = \mathcal{N}_{s'}(f_{\text{bim}})(x)$ . The decoding capabilities of each expert are then independently trained on these smashed data. In the second stage, the expert networks are frozen, and each sample  $x \in D_a$  is forward propagated with a random perturbation mechanism and noise scale to obtain smashed data  $\tilde{x}$ , which trains the gating network’s ability to select the appropriate experts for each input type.

The NaMoE model trained in this manner can effectively mitigate performance degradation caused by various perturbation strategies without requiring the adversary to make excessive assumptions about the target. Its adaptability to different forward perturbations will be demonstrated in Section 4. In practice, the adversary can establish multiple expert networks that cover the range of noise levels acceptable for effective LLM training (from minor perturbations to levels that completely destroy fine-tuning utility), thereby training a highly adaptable attack model.

**Table 1: Empirical hyperparameters for BiSR’s gradient-matching (GM) and smashed-data-matching (SM) enhancements targeting different LLMs.**

Model	Optimizer	Hyper Parameters						
		GM-epc	GM-lr	GM- $\beta$	GM- $\tau$	SM-epc	SM-lr	SM-wd
LLaMA2-7B	AdamW	18	0.09	0.85	1.2	800	0.005	0.02
GPT2-large	(0.9,	32	0.09	0.85	1.2	800	0.01	0.01
ChatGLM3-6B	0.999)	18	0.09	0.85	1.2	800	0.005	0.01

## 4 EXPERIMENTS

### 4.1 Setup

**Models.** Our experiments primarily focus on mainstream LLMs with decoder-only architectures, including GPT2-large [36], LLaMA2-chat-7B [47], and ChatGLM3-6B [16]. Due to hardware constraints, we employ 8-bit quantization during both the inference and fine-tuning of LLaMA2-chat-7B and ChatGLM3-6B, which, as shown in Appendix D.4, does not significantly impact attack performance. Additionally, to evaluate SIP, we conducted experiments on encoder-only models (BERT-large [13] and RoBERTa-large [28]) as well as an encoder-decoder model (FLAN-T5 [10]).

**Datasets.** To assess the vulnerability of split-FT in LLMs across various tasks, we utilize multiple datasets: QA datasets PIQA [5] and GSM8K [11], encyclopedic text dataset WikiText2-v1 [30], and the code dataset CodeAlpaca-20K [8] (details in Appendix B.0.1). To further investigate the attack performance of DRA methods on *sensitive information*, we modified the CNN-DailyMail News Text Summarization dataset [39] (details in Appendix B.0.2) to create the Sensitive Datasets (*Sensi-Series*): (1) SensiMarked, which annotates sensitive entities (names, dates, etc.) and focuses attack performance on them during evaluation; (2) SensiReplaced, created by substituting sensitive entities in SensiMarked with random, similar words to simulate a large-scale desensitized dataset; (3) SensiMasked, produced by masking all sensitive entities in SensiMarked with entity name tags for comparison. *In all experiments, SensiReplaced is used by default as  $D_a$ .*

**Evaluation Metrics.** To thoroughly evaluate data reconstruction attacks, we employ two main metrics. (1) ROUGE-L [27], our most stringent metric, measures sentence similarity based on the longest common subsequence, requiring strict adherence to both order and tokens. Scores range from 0 to 1, with 1 indicating perfect attack performance. (2) Meteor [4] assesses similarity using n-gram matching and incorporates WordNet for synonym recognition, allowing for more flexibility in word order and synonym use, making it our most lenient metric. Additional metrics and corresponding results are detailed in Appendix D.1.

**Evaluation Settings.** By default, a private-label SL setting with 6 Bottom blocks and 21 Trunk blocks (expressed as 6-21) is used for the three models. Attack performance was evaluated across steps of this split-FT system, capped at 600 steps. Attacks were conducted on 5 batches every 200 steps during FT to assess average performance. FT effectiveness was gauged by the perplexity of the LLM on the test dataset. Due to hardware constraints, a batch size of 2 was used, and LoRA was applied for PEFT. For SIP’s inversion model and NaMoE’s experts, a single-layer GRU (hidden size = 256, dropout = 0.1) was utilized. BRE’s optimization process used the best empirical hyperparameters for each LLM, as listed in Table 1.



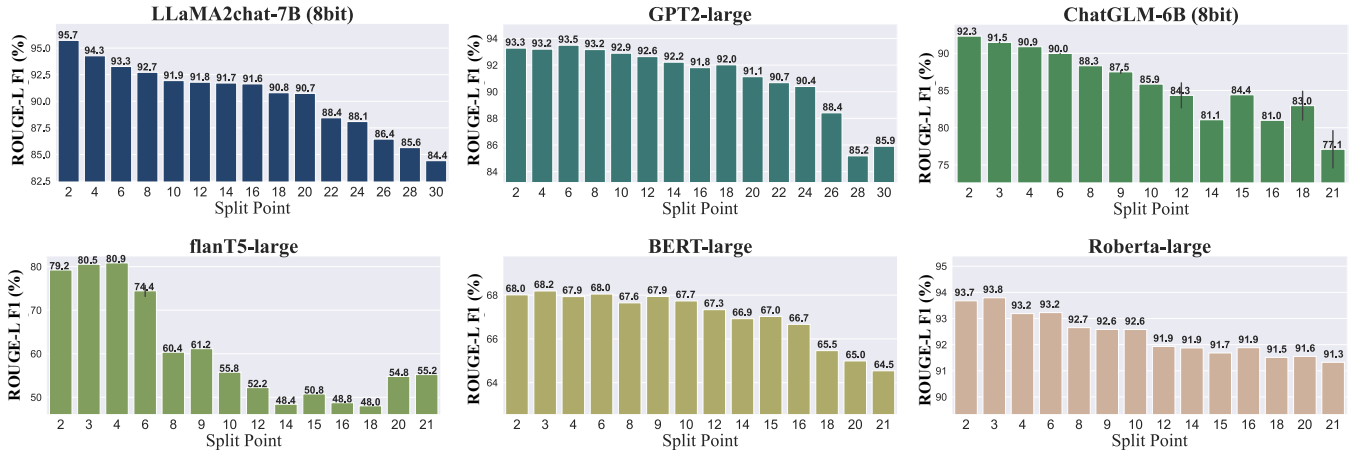


**Figure 7: Attack performance (ROUGE-L F1 %) of the proposed SIP on different LLMs using varying split points (e.g., split point=3 means blocks 0-2 are Bottom, and the output of the 3rd block is the attacked smashed data). For the encoder-decoder model flanT5, we consider the split point on the decoder, training the inverter to simultaneously recover the original inputs of the encoder and decoder from the decoder’s smashed data.**

Experiments were conducted on a single machine (PyTorch 2.0, using the Huggingface Transformers library) to simulate multi-party SL scenarios, all on Tesla V100-SXM2 GPUs (32GB). Main results were averaged over three random seeds to ensure reproducibility.

## 4.2 Evaluation on SIP

**Question 1.** *Is SIP effective across various models? How does the split point impact attack performance?*

SIP is applicable to all LLMs architectures. We evaluated its performance, measured by the ROUGE-L F1 score, on various LLM architectures to assess attack effectiveness on smashed data across different layers. These LLMs include decoder-only models (LLaMA2-chat-7B [47], GPT2-large [36], and ChatGLM3-6B [18]), encoder-only models (BERT-large [13] and Roberta-large [28]), and an encoder-decoder model (FLAN-T5 [10]). Using the PIQA dataset, which supports SFT tasks across these models (QA generation for encoder-decoder and decoder-only models, binary classification for encoder-only models), we trained the SIP inversion model on the validation set and evaluated its performance on an LLM fine-tuned with the PIQA training set. Note that for encoder-decoder models like T5, where the decoder depends on encoder outputs for cross-attention, the standard private-label SL architecture is unsuitable. Therefore, for comparison, we set the split point *only on the decoder*, using a concatenation of the encoder’s last hidden state and the decoder’s smashed data as input for the inversion model.

Figure 7 illustrates the attack performance of SIP on different LLMs at various split depths. SIP achieves high reconstruction performance, above 0.9, in shallow layers, especially in large-scale models like LLaMA2 and ChatGLM3. Deeper splits generally increase the difficulty of attacks. Compared to decoder-only models, masked language models such as Roberta and BERT show less intermediate output leakage.

**Table 2: Attack performance of SIP in cross-dataset attacks. Each row represents the ROUGE-L F1 score (%) of SIP attacks on LLaMA2 split-fine-tuned (cutlayer=6) on a specific dataset (with the inverter model trained on different datasets).**

Dataset	Inversion Model’s Training Dataset						
	CodeAl	GSM8K	PIQA	WikiT	SsMkd	SsRpl	SsMsk
CodeAl	95.78	59.25	61.13	55.18	67.54	65.02	67.11
	±0.15	±0.81	±1.43	±1.36	±0.85	±1.31	±1.13
GSM8K	70.71	93.85	74.53	91.41	88.05	85.27	83.73
	±0.43	±0.33	±1.86	±0.42	±0.33	±0.51	±1.14
PIQA	66.92	79.13	94.97	61.91	83.87	82.91	83.80
	±0.92	±1.42	±1.22	±0.80	±0.95	±0.72	±1.03
WikiT	50.42	60.20	56.19	91.41	96.96	95.81	88.15
	±1.22	±1.00	±1.07	±0.42	±0.36	±0.31	±2.32
SsMkd	39.07	52.63	42.62	75.36	97.54	95.57	74.17
	±1.59	±1.91	±1.98	±1.84	±0.80	±1.15	±2.78

**Question 2.** *What if the attack dataset  $D_a$  and the target dataset  $D_{c_i}$  are not sufficiently similar, i.e., if there is a distribution shift?*

To assess the generalizability of SIP, we evaluated its performance in cross-dataset attack tasks. Table 2 presents the performance of SIP in cross-dataset scenarios, where the inversion model is trained on one dataset and used to attack an LLM splitly fine-tuned on another dataset. We observed performance across various datasets: CodeAlpaca (CodeAl), Gsm8k, PIQA, WikiText-20K (WikiT), SensiMarked (SsMkd), and SensiReplaced (SsRpl). The results indicate that SIP demonstrates strong cross-dataset attack performance (with ROUGE-L scores consistently above 0.5). However, the gap between  $D_a$  and  $D_{c_i}$  does affect its effectiveness; for instance, performance tends to be lower on the CodeAlpaca dataset, which significantly differs from the others.

To further investigate SIP’s inversion patterns, we tested SIP inversion models trained on SensiReplaced and SensiMasked against

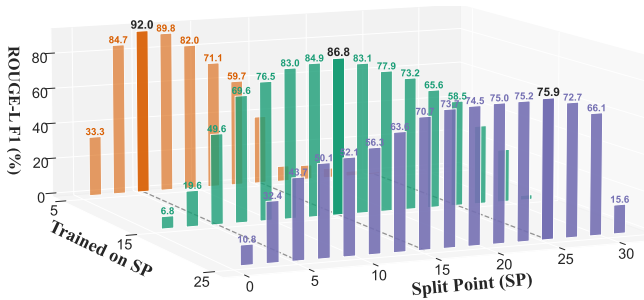


**Figure 8: Attack performance of SIP in cross-split-point attacks. The three sets of bar graphs represent ROUGE-L F1 scores (%) of SIP inversion models trained on the outputs of layers 5, 10, and 15 when attacking different layers of LLaMA2-chat-7B, with their performance at the split point they trained on emphasized.**

the SensiMarked dataset (see the right part of Table 2). The SensiReplaced-trained attacker, despite its training data having sensitive words replaced with similar entities, successfully recovers most sensitive entities in SensiMarked (0.95+). In contrast, the SensiMasked-trained attacker, trained with sensitive entities masked, shows much lower recovery performance (0.74). This underscores the importance of using complete sentences and sufficient entity words in the training data for effective sensitive entity attacks. It also indicates that SIP may prioritize learning specific token representations over decoding (inversion) rules for the LLM’s intermediate layer outputs. For further discussion on SIP’s inversion mechanism, see Appendix E.

**Question 3.** What if the simulated  $f_{btm}^-$  by the attacker is structurally inconsistent with the real  $f_{btm}$ ?

Figure 8 illustrates the cross-split-point attack performance of SIP, where the model is trained on one split setting (e.g., Split Point (SP) = 5, meaning the inversion model is trained on the output of the 5th block) and then used to attack a split-FT system with a different setting (e.g., SP = 10, meaning the Bottom segment has 10 blocks). This indicates that the attack model’s  $f_{btm}^-$  and the actual  $f_{btm}$  have varying layer counts. Results show that SIP possesses robust cross-layer attack capabilities, performing better on closer layers, and models trained on deeper layers exhibit better generalization across different model layers.

### 4.3 Evaluation on BiSR

**Question 4.** What are the advantages of BiSR in performance relative to other DRA methods across different LLMs?

Table 3 compares BiSR’s performance with various DRA methods attacking different LLMs fine-tuned on distinct datasets. We evaluated forward-DRA methods based on smashed data, including AE [54], which uses an autoencoder with an encoder structurally identical to the model’s Bottom but without pre-trained weights, and Embedding Inversion Attack (EIA)[20], which performs smashed-data matching through relaxed optimization on vocabulary and uses Euclidean Distance as the target. We also

evaluated backward-DRA methods based on gradient matching, including TAG[12] and LAMP [3].

It’s worth noting that, most of these baseline DRAs (EIA, DLG, TAG, and LAMP) were designed for *white-box* scenarios. For comparison, we adapted them to the *semi-white-box* SL setting by replacing the white-box model segments they access with the same model but with *pre-trained weights*, and marked their results with \*. For SIP and AE, the inversion model (GRU) was trained on SensiReplaced. For EIA, we followed He et al. [20], pretraining a Mapper network on SensiReplaced to map the targeted LLM hidden states back to a shallow layer (the first layer) before performing the attack. A two-layer MLP Mapper produced the best results for the LLMs considered. For gradient-based attacks (TAG and LAMP), we adapted them to the SL setting by reconstructing only the label  $y$ , given that the network input is known. All hyperparameters for each method and dataset were meticulously fine-tuned.

We present the outputs of BiSR at various stages: SIP-only showcases the initial output from the learning-based inversion model’s direct attack, while BiSR (b) and BiSR (f) respectively represent the results enhanced with gradient matching and smashed-data matching based on SIP. BiSR (b+f) indicates the sequentially enhanced results using BRE, with backward enhancement followed by forward enhancement. As the table illustrates, for larger models, purely optimization-based methods like TAG and EIA are limited by extensive search spaces, resulting in a lower reconstruction performance ceiling. It is worth noting that in the considered setup, LAMP did not achieve an advantage over TAG. This is because when applying gradient attacks in SL scenarios, there is no issue of sentence order. As a result, the token reorder operation in LAMP does not provide a substantial benefit. The learning-based SIP-only approach produces high-quality recovered sentences without any iteration steps but suffers performance drawbacks when significant discrepancies exist between  $D_a$  and the target data (e.g., CodeAlpaca). BiSR, integrating learning-based and optimization-based approaches, achieves significantly optimal recovery performance. This effectiveness stems from SIP providing an excellent starting point for optimization, thereby facilitating the bidirectional optimization process to more effectively find the global optimum.

**Question 5.** Does the Not-too-far Assumption hold in practice?

To validate the Not-too-far Assumption, we assessed various DRAs in scenarios where the client does not initiate FT from the pre-trained weights provided by the server. We simulated this by: (1) Attacking a LLaMA2-chat-7B model that was splitly fine-tuned on PIQA, with the client performing FT on the Bottom and Top parts for several steps on CodeAlpaca-20K beforehand (pre-FT), diverging them from the pre-trained state; (2) Attacking a well-fine-tuned model, specifically the LLaMA2-based Vicuna-v1.5-7B [56]. As shown in Table 4, when the client’s model portions diverge further from the pre-trained states, with the L2-norm of their tunable parameters (LoRA Adapters) increasing from 19.59 to 32.89, the attack performance of BiSR and other DRAs does not exhibit a decline. Even when attacking Vicuna while semi-white-box accessing LLaMA2’s weights, the performance remains unaffected. Thus, Assumption 1 holds empirically. Furthermore, we compared DRA

**Table 3: Performance of BiSR on various LLMs fine-tuned on different datasets (ROUGE-L F1 Score %) compared to alternative methods. Experiments utilized split points set at 6-27, with SensiReplaced serving as the auxiliary dataset  $D_a$ . The best results for each configuration are highlighted in bold, with the second best results underlined.**

Model	Methods	Split Fine-tuning Datasets									
		SensiMkd		Codealpaca		Gsm8k		PIQA		WikiText	
		RougeL-F	Meteor	RougeL-F	Meteor	RougeL-F	Meteor	RougeL-F	Meteor	RougeL-F	Meteor
LLaMA2	AE	49.99±0.34	46.99±1.62	60.31±0.48	62.09±0.74	42.32±0.33	46.41±0.83	32.63±1.29	29.78±1.71	47.15±0.67	41.05±0.92
	EIA*	83.06±4.92	77.98±5.35	54.00±2.90	49.83±3.31	59.97±3.78	62.22±3.19	57.86±0.46	65.93±1.45	83.42±1.25	81.50±0.22
	TAG*	80.22±1.47	79.61±1.25	84.94±0.25	85.34±0.89	82.40±1.93	84.45±1.01	77.05±2.30	78.10±1.75	74.36±1.16	72.68±0.75
	LAMP*	79.13±0.66	78.55±0.26	83.51±0.13	85.11±0.17	83.23±0.14	83.82±0.31	76.50±1.03	76.22±1.09	74.23±0.89	72.40±0.86
	SIP-only	95.66±0.98	96.37±1.18	65.08±1.12	66.67±0.89	85.37±0.75	88.05±0.25	82.83±0.64	96.57±0.26	95.90±0.41	89.06±0.54
	BiSR(b)	96.80±0.78	97.42±0.76	83.02±1.12	85.65±0.83	90.82±0.69	93.80±1.03	89.34±0.67	97.10±0.32	96.31±0.38	94.65±0.32
	BiSR(f)	98.70±0.58	98.94±0.34	86.93±0.88	94.39±1.22	94.59±0.40	95.96±1.05	92.30±1.14	99.01±0.29	98.09±0.33	97.70±0.19
	BiSR	<b>99.64±0.26</b>	<b>99.47±0.42</b>	<b>92.62±0.77</b>	<b>96.58±0.14</b>	<b>95.98±0.18</b>	<b>97.71±0.06</b>	<b>95.84±0.15</b>	<b>99.46±0.14</b>	<b>98.49±0.27</b>	<b>98.03±0.17</b>
GPT2-large	AE	75.47±0.31	78.04±1.21	85.66±0.36	90.23±0.28	73.20±1.02	88.00±0.52	64.11±0.82	69.32±1.55	82.55±4.96	63.04±2.36
	EIA*	85.15±3.11	61.35±6.70	50.54±7.12	39.76±4.66	65.75±4.84	57.29±7.51	60.59±2.10	57.45±2.64	81.50±0.56	71.17±2.23
	TAG*	62.32±5.48	45.99±4.74	77.62±1.08	74.82±1.48	78.63±1.19	75.11±1.40	71.04±1.92	67.71±0.82	68.47±0.86	67.67±0.29
	LAMP*	60.29±0.24	48.33±0.60	76.48±0.18	75.01±0.14	75.16±0.27	67.33±0.31	68.59±0.44	64.48±0.24	67.57±0.27	66.34±0.11
	SIP-only	80.84±0.75	90.69±0.27	88.77±0.32	93.22±0.38	93.19±0.17	92.85±0.86	78.41±1.25	84.84±1.04	93.53±0.34	78.04±4.68
	BiSR(b)	88.16±0.74	92.87±0.24	94.81±0.35	96.48±0.06	95.76±0.21	95.12±0.71	91.14±0.34	93.41±0.15	97.28±0.75	82.26±3.66
	BiSR(f)	95.07±0.60	97.43±0.24	97.22±0.81	99.05±0.28	99.06±0.29	99.30±0.13	92.30±1.12	96.17±0.63	99.71±0.26	83.91±3.71
	BiSR	<b>95.20±0.83</b>	<b>97.46±0.43</b>	<b>97.16±0.55</b>	<b>99.11±0.11</b>	<b>99.14±0.11</b>	<b>99.38±0.01</b>	<b>92.64±0.70</b>	<b>99.79±0.29</b>	<b>98.06±3.89</b>	
Chat-GLM3	AE	66.36±1.12	62.08±0.67	68.89±0.57	64.22±0.69	62.61±0.91	64.86±0.80	48.94±0.44	41.83±1.82	65.85±1.08	59.06±2.21
	EIA*	61.53±13.47	62.42±15.69	12.14±1.33	10.43±1.66	11.41±0.25	12.80±1.04	29.50±6.14	27.84±6.35	26.65±0.15	26.76±1.61
	TAG*	60.86±1.97	59.22±2.04	77.55±0.98	81.75±2.49	79.23±1.64	83.41±3.09	67.30±0.52	68.30±1.02	66.04±1.17	65.42±0.82
	LAMP*	39.20±0.47	36.01±0.13	76.27±0.40	78.28±0.13	77.60±0.26	81.34±0.33	66.95±0.47	67.22±0.28	67.18±0.52	65.59±0.21
	SIP-only	93.78±1.14	94.75±1.20	63.81±1.40	61.92±2.45	77.00±0.88	79.74±0.49	92.57±0.30	92.37±0.60	82.34±0.69	86.13±0.37
	BiSR(b)	94.96±1.29	95.54±1.02	<b>86.96±0.42</b>	83.13±0.74	90.59±0.63	90.97±0.42	94.45±0.23	94.68±0.17	<b>93.11±0.82</b>	93.43±0.74
	BiSR(f)	100.00±0.00	99.99±0.01	86.64±1.48	90.66±1.05	89.92±1.07	90.13±0.68	<b>99.72±0.10</b>	<b>99.76±0.04</b>	86.12±1.72	95.74±0.34
	BiSR	<b>100.00±0.00</b>	<b>99.99±0.01</b>	86.64±1.55	<b>93.37±0.61</b>	<b>90.90±0.31</b>	<b>96.09±0.14</b>	99.71±0.09	99.74±0.05	86.52±1.97	<b>96.38±0.38</b>

**Table 4: Validation of the Not-too-far Assumption: comparing the attack performance (ROUGE-L F1 Score %) of different DRAs on LLaMA2-chat-7B with varying pre-fine-tuning steps, and on a well-fine-tuned model Vicuna-v1.5-7B.**

DRA Methods	Pre-fine-tuning Steps						Cross-model
	0	4800	9600	14400	19200	24000	Vicuna
EIA	49.15 ± 2.27	50.89 ± 4.32	57.49 ± 6.50	53.50 ± 6.99	62.96 ± 3.53	62.17 ± 4.40	48.59 ± 15.51
TAG	75.36 ± 4.24	69.62 ± 2.13	70.14 ± 1.42	70.46 ± 0.75	70.20 ± 1.94	70.04 ± 2.63	73.24 ± 1.67
SIP	80.50 ± 1.78	77.99 ± 2.05	81.23 ± 2.75	81.14 ± 1.89	82.38 ± 1.56	82.63 ± 1.80	82.27 ± 2.67
BiSR(b)	88.26 ± 2.81	89.09 ± 1.66	88.70 ± 2.04	88.14 ± 0.62	89.58 ± 2.50	89.19 ± 1.07	89.39 ± 1.74
BiSR(f)	82.91 ± 2.10	79.29 ± 1.89	81.17 ± 2.98	79.42 ± 1.95	80.06 ± 2.26	80.15 ± 2.12	95.66 ± 0.77
BiSR(b+f)	93.22 ± 1.37	91.73 ± 3.30	92.02 ± 4.07	92.11 ± 2.86	95.56 ± 0.63	95.05 ± 0.40	96.49 ± 0.55
LoRA L2-Norm	19.59 ± 0.01	26.29 ± 0.08	28.18 ± 0.18	29.89 ± 0.21	31.44 ± 0.23	32.89 ± 0.29	-

for language and vision models in Appendix F, suggesting that The Not-too-far may be uniquely applicable to language models.

#### 4.4 Evaluation on BiSR’s Noise Adaptability

**Question 6.** How does BiSR adapt to various forward perturbation mechanisms?

We evaluated three representative non-cryptographic privacy preservation techniques for SL, which mitigate privacy leakage by perturbing intermediate results during forward propagation. The selected mechanisms include: Embedding- $d_{\chi P}$  [7], which perturbs sentence embeddings in language models; Smashed-Data-DP [15, 45, 53], which injects noise directly into smashed data; and NoPeek [50], which restricts the relevance of intermediate data to the input.

**Embedding- $d_{\chi P}$ .** Table 5 presents the results of embedding- $d_{\chi P}$  [7] tests conducted using the LLaMA2-chat-7B model. The model was fine-tuned on PIQA with  $d_{\chi P}$  noise applied to the Bottom part’s embedding layer. The noise scale is defined by the relative parameter  $\epsilon' = \epsilon/n$ , where  $n$  is the dimensionality of the model’s hidden states and  $\epsilon$  is the original  $d_{\chi P}$ -Privacy parameter. A smaller  $\epsilon'$  indicates stronger perturbations. In this experiment, the NaMoE model comprised four experts with  $\epsilon'$  values of  $+\infty$ , 0.08, 0.38, and 0.21, each using a GRU with 256 hidden units. We trained the experts for 15 epochs and the gating network for 10 epochs on SensiReplaced. As shown in Table 5, the NaMoE inversion model consistently outperforms a standard, noise-unaware GRU across various noise scales, even without strictly following the noise scales used by the expert models. Notably, even when model performance

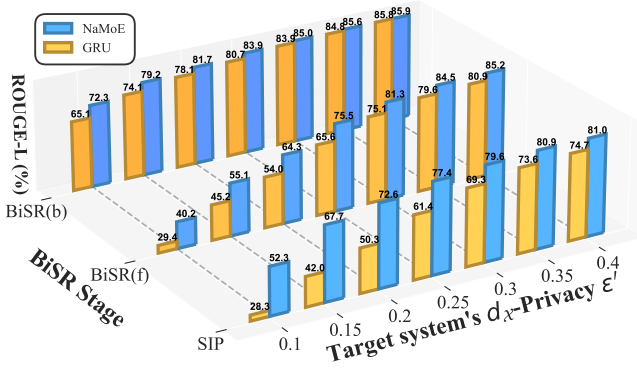


**Figure 9: Comparison of attack performance at different stages of BiSR when using NaMoE versus a standard GRU-based SIP for initial reconstruction under varying scales of  $d\chi^P$  noise. Each set of bars represents the ROUGE-L F1 Score (%) of the attack method when the target system applies a specific scale of  $d\chi^P$  perturbation.**

**Table 5: Performance comparison (ROUGE-L F1 Score %  $\uparrow$ ) of BiSR against various DRAs under embedding- $d\chi^P$  perturbations, alongside a comparison between the NaMoE model and a standard noise-unaware GRU model. LLM utility was assessed using test perplexity ( $\downarrow$ ). Experiments were conducted with the LLaMA2-chat-7B model and the PIQA dataset, with SensiReplaced serving as the auxiliary dataset  $D_a$ .**

Methods	$d\chi^P-\epsilon'$						
	0.4	0.35	0.30	0.25	0.20	0.15	0.10
EIA*	51.98 $\pm 2.72$	54.45 $\pm 2.72$	51.80 $\pm 2.84$	43.66 $\pm 0.35$	42.33 $\pm 0.45$	32.25 $\pm 3.83$	17.56 $\pm 0.23$
TAG*	73.95 $\pm 0.65$	73.26 $\pm 0.25$	71.86 $\pm 0.35$	69.57 $\pm 0.96$	68.56 $\pm 0.97$	68.36 $\pm 1.24$	63.19 $\pm 1.16$
SIP (GRU)	74.73 $\pm 0.56$	73.59 $\pm 1.16$	69.26 $\pm 1.89$	61.40 $\pm 2.16$	50.29 $\pm 1.61$	41.98 $\pm 1.21$	28.34 $\pm 2.08$
SIP (NaMoE)	80.96 $\pm 0.89$	80.93 $\pm 0.80$	79.62 $\pm 0.23$	77.44 $\pm 0.77$	72.56 $\pm 0.54$	67.65 $\pm 0.64$	52.31 $\pm 1.57$
BiSR(b)	85.95 $\pm 1.42$	85.58 $\pm 1.82$	85.01 $\pm 1.00$	83.86 $\pm 0.93$	81.71 $\pm 0.50$	79.20 $\pm 0.37$	72.34 $\pm 0.70$
BiSR(b+f)	91.06 $\pm 0.16$	89.82 $\pm 0.40$	86.74 $\pm 0.36$	79.78 $\pm 0.58$	67.65 $\pm 0.95$	58.64 $\pm 0.73$	42.26 $\pm 1.45$
Test PPL	31.82 $\pm 0.63$	37.71 $\pm 2.33$	57.00 $\pm 1.51$	61.86 $\pm 2.34$	48.44 $\pm 1.48$	47.51 $\pm 1.88$	138.86 $\pm 4.31$

collapses (test perplexity > 100) at  $\epsilon' = 0.1$ , NaMoE still achieves a recovery performance above 0.5. The advantages of NaMoE over GRU and its impact on subsequent optimization-based attacks are more clearly illustrated in Figure 9. It is also important to note that optimization-based methods relying on smashed data matching, such as EIA and BiSR(b+f), are more sensitive to noise than the learning-based SIP. Under high noise levels, the (f) phase of BRE can degrade SIP performance, while gradient-based DRAs remain largely unaffected.

**Table 6: Performance comparison (ROUGE-L F1 Score %  $\uparrow$ ) of BiSR versus various DRAs and LLM utility (test perplexity  $\downarrow$ ) under smashed-data-DP perturbations. The experiments used the LLaMA2-chat-7B model with split points 6-27 and the PIQA dataset. The *attack-deeper* strategy was employed, with the NaMoE model trained on SensiReplaced and targeting the model’s 9th block’s output.**

Methods	DP- $\epsilon'$						
	7.0	6.5	6.0	5.5	5.0	4.5	4.0
EIA*	34.27 $\pm 1.49$	31.71 $\pm 1.60$	27.00 $\pm 0.60$	23.23 $\pm 0.63$	18.27 $\pm 0.59$	15.83 $\pm 0.46$	12.62 $\pm 0.62$
TAG*	67.05 $\pm 0.85$	66.66 $\pm 0.51$	65.72 $\pm 0.56$	63.01 $\pm 0.32$	61.12 $\pm 0.88$	60.78 $\pm 0.71$	60.78 $\pm 0.71$
SIP (GRU)	31.58 $\pm 1.18$	27.23 $\pm 0.96$	22.73 $\pm 2.24$	18.97 $\pm 0.35$	14.90 $\pm 0.61$	9.78 $\pm 1.06$	7.64 $\pm 0.50$
SIP (NaMoE)	55.13 $\pm 1.05$	52.07 $\pm 1.39$	49.11 $\pm 1.27$	45.75 $\pm 1.32$	39.85 $\pm 0.86$	33.59 $\pm 0.77$	26.67 $\pm 1.27$
BiSR(b)	76.29 $\pm 1.65$	74.39 $\pm 1.18$	72.27 $\pm 0.75$	68.48 $\pm 0.87$	64.95 $\pm 0.95$	61.43 $\pm 0.64$	56.41 $\pm 1.63$
BiSR(b+f)	67.90 $\pm 2.13$	65.85 $\pm 1.76$	63.41 $\pm 1.57$	58.88 $\pm 1.66$	55.60 $\pm 2.02$	52.37 $\pm 1.63$	48.09 $\pm 2.69$
Test PPL	31.80 $\pm 0.66$	35.42 $\pm 0.48$	40.18 $\pm 0.35$	49.43 $\pm 0.82$	68.18 $\pm 1.01$	112.71 $\pm 2.29$	269.10 $\pm 67.23$

**Smashed-data-DP.** Table 6 displays the performance of BiSR compared to other DRA methods across various scales of smashed-data-DP [15, 45, 53]. We define  $\epsilon^* = \epsilon/G$  as the relative DP parameter, where  $G$  is the clipping threshold (fixed at 2000 for this experiment), and we evaluated the performance of BiSR on LLaMA2-chat-7B model and the PIQA dataset. The NaMoE model here also includes three experts, corresponding to  $\epsilon^* = +\infty$ ,  $\epsilon^* = 3.0$ ,  $\epsilon^* = 5.0$ , and  $\epsilon^* = 8.0$ . It is important to note that directly training the inversion model on heavily perturbed smashed data is challenging. To address this, we employed an *attack-deeper strategy*: the curious server targets hidden states a few layers deeper within the Trunk instead of at the cut layer. This approach leverages the LLM’s noise adaptability—during noisy training, the LLM reduces perturbation impact, leading to decreased noise in hidden states after several LLM blocks. Thus, although the cut layer was set at layer 6 in LLaMA2 (where noise is added), we trained the NaMoE model on layer 9, significantly reducing training difficulty. As shown in Table 6, NaMoE exhibits stronger adaptability than the GRU, maintaining recovery performance above 0.2 even under extreme conditions. However, forward optimization (f) becomes ineffective when noise is directly added to smashed data.

**NoPeek.** Since NoPeek’s perturbation method optimizes regularization terms rather than directly adding random noise, the evaluation approach and NaMoE model training differ significantly from the previous methods. We employed GPT2-large with an increased batch size (=6) to ensure distance correlation was effective. Instead of attacking 5 batches every 200 steps, we reduced the attack frequency to 5 batches every 1200 steps to allow the regularization term to stabilize—posing a greater challenge to the attacker, as earlier attacks typically yield better results. A simulation strategy was employed to train the noise-aware NaMoE model (see Appendix

**Table 7: Adaptability of BiSR to NoPeek-based perturbations. Experiments were conducted on the GPT2-large model and the PIQA dataset, with the NaMoE inversion model trained on SensiReplaced.**

Methods	NoPeek- $\alpha 2$						
	10	30	50	70	90	110	130
EIA*	14.49 $\pm 1.16$	13.17 $\pm 0.51$	12.57 $\pm 1.33$	12.46 $\pm 0.96$	12.02 $\pm 0.96$	11.43 $\pm 0.9$	10.90 $\pm 1.40$
TAG*	66.03 $\pm 0.86$	63.92 $\pm 1.11$	63.02 $\pm 1.21$	62.83 $\pm 0.36$	53.05 $\pm 1.10$	53.16 $\pm 1.55$	54.76 $\pm 2.16$
SIP (GRU)	59.45 $\pm 0.03$	54.07 $\pm 1.20$	38.68 $\pm 0.40$	32.88 $\pm 4.90$	17.43 $\pm 3.62$	11.38 $\pm 2.14$	7.19 $\pm 2.36$
SIP (NaMoE)	63.74 $\pm 1.35$	56.32 $\pm 1.03$	48.08 $\pm 2.39$	39.53 $\pm 0.01$	28.94 $\pm 2.89$	20.56 $\pm 3.50$	17.79 $\pm 3.69$
BiSR(b)	81.43 $\pm 0.11$	77.47 $\pm 2.59$	64.62 $\pm 2.34$	55.06 $\pm 3.34$	41.72 $\pm 3.27$	35.61 $\pm 0.80$	33.52 $\pm 0.75$
BiSR(b+f)	81.38 $\pm 0.15$	75.28 $\pm 2.95$	61.29 $\pm 3.61$	56.34 $\pm 0.34$	40.86 $\pm 3.41$	34.03 $\pm 0.20$	32.68 $\pm 0.79$
Test PPL	5.26 $\pm 0.08$	9.89 $\pm 2.74$	30.31 $\pm 1.37$	51.42 $\pm 24.16$	60.01 $\pm 11.35$	82.46 $\pm 18.06$	93.07 $\pm 7.47$

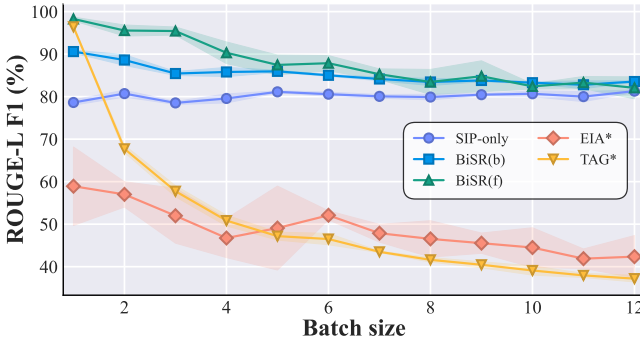


**Figure 10: The impact of batch size on the attack performance of BiSR and other DRAs, tested on the GPT2-large and the PIQA dataset (with the maximum sentence length truncated to 128). Error bars are plotted as shaded regions.**

D.2). Additionally, the *attack-deeper* approach was applied, targeting layer 8 of GPT2-large. As shown in Table 7, NaMoE demonstrates adaptability to NoPeek perturbations, outperforming the GRU. Notably, the purely gradient-based DRA method, TAG, also experienced performance degradation under NoPeek perturbations.

#### 4.5 Impact of Batch Size

The minibatch size is a critical factor frequently examined in DRA literature, particularly in gradient-based DRAs, as gradient averaging across batches can complicate the success of attacks. The optimization-based procedures in BRE are similarly impacted by this factor. Although batch sizes in LLM scenarios are generally limited by resource constraints—especially in the SL scenario discussed in this paper—we evaluated the performance of BiSR and various baselines as the batch size increased. These experiments were conducted using the GPT2-large model and the PIQA dataset, with a maximum sentence length of 128 to allow for larger batch sizes while keeping the experimental setup consistent.

As illustrated in Fig. 10, increasing the batch size significantly diminishes the effectiveness of both optimization-based attacks, i.e., EIA and TAG, while the learning-based SIP-only approach remains unaffected. Due to the inclusion of forward and backward optimizations in BRE, BiSR also experiences reduced performance at larger batch sizes. However, under the hyperparameter settings detailed in Table 1, both BiSR(b) and BiSR(f) still outperform SIP even with larger batch sizes (though a higher number of BRE epochs may adversely affect performance in this context). This is because BiSR benefits from SIP’s initialization, leveraging its learning-based strengths to handle larger batches more effectively. This results in lower search difficulty during optimization-based attacks, thereby providing greater robustness to larger batch sizes compared to other baselines.

Additionally, it is important to note that while increasing the batch size can effectively reduce DRA risks, it also demands higher computational resources, leading to a trade-off between privacy protection and resource expenditure. Besides batch size, other factors (e.g., quantization, split points) also affect DRA performance. For additional experimental results, please refer to Appendix D.

## 5 RELATED WORK

**Split Learning for LLMs.** SL is a distributed learning technique that partitions an entire model into consecutive chunks of layers among various parties [19, 49]. By selecting appropriate split points, the model’s architecture and weights can be partially concealed from each party. Leveraging SL, FedBERT [44] partitions the BERT model for split-based pretraining, while PrivateLoRA [51] splits LLMs and low-rank adapter matrices for split-based model fine-tuning. SAP [40] proposed an SL framework for fine-tuning LLMs, adding perturbations to the smashed data to enhance privacy.

**Data Reconstruction Attacks on SL.** Considering the two phases of intermediate data transmission in SL, DRAs on SL can be divided into *forward DRAs* [22, 54] and *backward DRAs* [12, 57], targeting smashed data during forward propagation and gradients from backward propagation, respectively. DRAs can be further categorized into *learning-based DRAs* and *optimization-based DRAs* based on the attack techniques. Learning-based DRAs involve training an inversion model on auxiliary data to map intermediate representations to the original input [21, 54]. Optimization-based DRAs treat data reconstruction as non-convex optimization problems [24]. EIA [42] trains a mapper to project deep embeddings to shallow ones, then optimizes the input to match the smashed data with the shallow output. Gradient attack methods like DLG [57] and TAG [12] construct dummy data to match observed gradients, while LAMP [3] adds token reordering and language priors to the search, though these are largely ineffective in SL scenarios. All these methods attack from a single direction.

## 6 CONCLUSION

This paper highlights the vulnerabilities of split-based FT for LLMs and proposes an attack scheme, BiSR, tailored to the characteristics of this scenario. SIP is designed for attackers aware of pre-trained weights, and experiments demonstrate the recoverability of intermediate outputs during the FT process of mainstream generative LLMs. BRE combines forward SIP with backward gradient matching

attacks, significantly enhancing attack performance in scenarios such as cross-dataset attacks and forward noise addition. Additionally, based on observations of the language model's adaptability to forward random noise, NaMoE is proposed to enable DRA attackers to better adapt to unknown forward noise, further strengthening attack performance under perturbations.

Therefore, the direct application of SL to LLM-FT carries significant security risks. We aim to spur future research to either address these vulnerabilities or develop protective measures.

## 7 ACKNOWLEDGEMENT

We thank the anonymous reviewers for their valuable comments. We would like to extend our gratitude to Xuhong Zhang, Qiang Yang for their insightful suggestions. This research is partially supported by the Major Key Project of PCL (PCL2023A09), the NSFC under No. 62402418, and the Ningbo Key Research and Development Program under No. 2024Z115.

## REFERENCES

- [1] Martin Abadi, Andy Chu, Ian J. Goodfellow, H. Brendan McMahan, Ilya Mironov, Kunal Talwar, and Li Zhang. 2016. Deep Learning with Differential Privacy. In *Proceedings of the 2016 ACM SIGSAC Conference on Computer and Communications Security, Vienna, Austria, October 24–28, 2016*, Edgar R. Weippl, Stefan Katzenbeisser, Christopher Kruegel, Andrew C. Myers, and Shai Halevi (Eds.). ACM, New York, NY, USA, 308–318. <https://doi.org/10.1145/2976749.2978318>
- [2] Ali Abedi and Shehroz S Khan. 2024. FedSL: Federated split learning on distributed sequential data in recurrent neural networks. *Multimedia Tools and Applications* 83, 10 (2024), 28891–28911.
- [3] Mislav Balunovic, Dimitar I. Dimitrov, Nikola Jovanovic, and Martin T. Vechev. 2022. LAMP: Extracting Text from Gradients with Language Model Priors. In *Advances in Neural Information Processing Systems 35: Annual Conference on Neural Information Processing Systems 2022, NeurIPS 2022, New Orleans, LA, USA, November 28 - December 9, 2022*, Sanmi Koyejo, S. Mohamed, A. Agarwal, Danielle Belgrave, K. Cho, and A. Oh (Eds.). Curran Associates, Inc., 7641–7654. [http://papers.nips.cc/paper\\_files/paper/2022/hash/32375260090404f907ceae19f3564a7e-Abstract-Conference.html](http://papers.nips.cc/paper_files/paper/2022/hash/32375260090404f907ceae19f3564a7e-Abstract-Conference.html)
- [4] Satanjeev Banerjee and Alon Lavie. 2005. METEOR: An Automatic Metric for MT Evaluation with Improved Correlation with Human Judgments. In *Proceedings of the Workshop on Intrinsic and Extrinsic Evaluation Measures for Machine Translation and/or Summarization@ACL 2005, Ann Arbor, Michigan, USA, June 29, 2005*, Jade Goldstein, Alon Lavie, Chin-Yew Lin, and Clare R. Voss (Eds.). Association for Computational Linguistics, 65–72. <https://aclanthology.org/W05-0909/>
- [5] Yonatan Bisk, Rowan Zellers, Ronan Le Bras, Jianfeng Gao, and Yejin Choi. 2020. PIQA: Reasoning about Physical Commonsense in Natural Language. In *The Thirty-Fourth AAAI Conference on Artificial Intelligence, AAAI 2020, The Thirty-Second Innovative Applications of Artificial Intelligence Conference, IAAI 2020, The Tenth AAAI Symposium on Educational Advances in Artificial Intelligence, EAAI 2020, New York, NY, USA, February 7–12, 2020*. AAAI Press, 7432–7439. <https://doi.org/10.1609/AAAI.V34I05.6239>
- [6] Tom B. Brown, Benjamin Mann, Nick Ryder, Melanie Subbiah, Jared Kaplan, Prafulla Dhariwal, Arvind Neelakantan, Pranav Shyam, Girish Sastry, Amanda Askell, Sandhini Agarwal, Ariel Herbert-Voss, Gretchen Krueger, Tom Henighan, Rewon Child, Aditya Ramesh, Daniel M. Ziegler, Jeffrey Wu, Clemens Winter, Christopher Hesse, Mark Chen, Eric Sigler, Mateusz Litwin, Scott Gray, Benjamin Chess, Jack Clark, Christopher Berner, Sam McCandlish, Alec Radford, Ilya Sutskever, and Dario Amodei. 2020. Language Models are Few-Shot Learners. In *Advances in Neural Information Processing Systems 33: Annual Conference on Neural Information Processing Systems 2020, NeurIPS 2020, December 6–12, 2020, virtual*, Hugo Larochelle, Marc'Aurelio Ranzato, Raia Hadsell, Maria-Florina Balcan, and Hsuan-Tien Lin (Eds.). <https://proceedings.neurips.cc/paper/2020/hash/1457c0d6bfc4967418bf8ac142f64a-Abstract.html>
- [7] Konstantinos Chatzikokolakis, Miguel E. Andrés, Nicolás Emilio Bordenabe, and Catuscia Palamidessi. 2013. Broadening the Scope of Differential Privacy Using Metrics. In *Privacy Enhancing Technologies - 13th International Symposium, PETS 2013, Bloomington, IN, USA, July 10–12, 2013. Proceedings (Lecture Notes in Computer Science, Vol. 7981)*, Emiliano De Cristofaro and Matthew K. Wright (Eds.). Springer, Berlin, Heidelberg, 82–102. [https://doi.org/10.1007/978-3-642-39077-7\\_5](https://doi.org/10.1007/978-3-642-39077-7_5)
- [8] Sahil Chaudhary. 2023. Code Alpaca: An Instruction-following LLaMA model for code generation. <https://github.com/sahil280114/codealpaca>.
- [9] Yiqiang Chen, Teng Zhang, Xinlong Jiang, Qian Chen, Chenlong Gao, and Wu-liang Huang. 2023. FedBone: Towards Large-Scale Federated Multi-Task Learning. *CoRR abs/2306.17465* (2023). <https://doi.org/10.48550/ARXIV.2306.17465> arXiv:2306.17465
- [10] Hyung Won Chung, Le Hou, Shayne Longpre, Barret Zoph, Yi Tay, William Fedus, Eric Li, Xuezhi Wang, Mostafa Dehghani, Siddhartha Brahma, Albert Webson, Shixiang Shane Gu, Zhuyun Dai, Mirac Suzgun, Xinyun Chen, Aakanksha Chowdhery, Sharan Narang, Gaurav Mishra, Adams Yu, Vincent Zhao, Yanping Huang, Andrew Dai, Hongkun Yu, Slav Petrov, Ed H. Chi, Jeff Dean, Jacob Devlin, Adam Roberts, Denny Zhou, Quoc V. Le, and Jason Wei. 2022. Scaling Instruction-Finetuned Language Models. <https://doi.org/10.48550/ARXIV.2210.11416>
- [11] Karl Cobbe, Vineet Kosaraju, Mohammad Bavarian, Mark Chen, Heewoo Jun, Lukasz Kaiser, Matthias Plappert, Jerry Tworek, Jacob Hilton, Reiichiro Nakano, Christopher Hesse, and John Schulman. 2021. Training Verifiers to Solve Math Word Problems. *CoRR abs/2110.14168* (2021). arXiv:2110.14168 <https://arxiv.org/abs/2110.14168>
- [12] Jieren Deng, Yijue Wang, Ji Li, Chonghong Wang, Chao Shang, Hang Liu, Sanguthevar Rajasekaran, and Caiwen Ding. 2021. TAG: Gradient Attack on Transformer-based Language Models. In *Findings of the Association for Computational Linguistics: EMNLP 2021, Virtual Event / Punta Cana, Dominican Republic, 16–20 November, 2021*, Marie-Francine Moens, Xuanjing Huang, Lucia Specia, and Scott Wen-tau Yih (Eds.). Association for Computational Linguistics, 3600–3610. <https://doi.org/10.18653/V1/2021.FINDINGS-EMNLP.305>
- [13] Jacob Devlin, Ming-Wei Chang, Kenton Lee, and Kristina Toutanova. 2019. BERT: Pre-training of Deep Bidirectional Transformers for Language Understanding. In *Proceedings of the 2019 Conference of the North American Chapter of the Association for Computational Linguistics: Human Language Technologies, NAACL-HLT 2019, Minneapolis, MN, USA, June 2–7, 2019, Volume 1 (Long and Short Papers)*, Jill Burstein, Christy Doran, and Thamar Solorio (Eds.). Association for Computational Linguistics, 4171–4186. <https://doi.org/10.18653/V1/N19-1423>
- [14] Alexey Dosovitskiy, Lucas Beyer, Alexander Kolesnikov, Dirk Weissenborn, Xi-aohua Zhai, Thomas Unterthiner, Mostafa Dehghani, Matthias Minderer, Georg Heigold, Sylvain Gelly, Jakob Uszkoreit, and Neil Houlsby. 2021. An Image is Worth 16x16 Words: Transformers for Image Recognition at Scale. In *9th International Conference on Learning Representations, ICLR 2021, Virtual Event, Austria, May 3–7, 2021*. OpenReview.net. <https://openreview.net/forum?id=YicbFdNTTy>
- [15] Minxin Du, Xiang Yue, Sherman S. M. Chow, Tianhao Wang, Chenyu Huang, and Huan Sun. 2023. DP-Forward: Fine-tuning and Inference on Language Models with Differential Privacy in Forward Pass. In *Proceedings of the 2023 ACM SIGSAC Conference on Computer and Communications Security, CCS 2023, Copenhagen, Denmark, November 26–30, 2023*, Weizhi Meng, Christian Damsgaard Jensen, Cas Cremers, and Engin Kirda (Eds.). ACM, New York, NY, USA, 2665–2679. <https://doi.org/10.1145/3576915.3616592>
- [16] Zhengxiao Du, Yujie Qian, Xiao Liu, Ming Ding, Jiezhong Qiu, Zhilin Yang, and Jie Tang. 2022. GLM: General Language Model Pretraining with Autoregressive Blank Infilling. In *Proceedings of the 60th Annual Meeting of the Association for Computational Linguistics (Volume 1: Long Papers), ACL 2022, Dublin, Ireland, May 22–27, 2022*, Smaranda Muresan, Preslav Nakov, and Aline Villavicencio (Eds.). Association for Computational Linguistics, 320–335. <https://doi.org/10.18653/V1/2022.ACL-LONG.26>
- [17] Oluwaseyi Feyisetan, Borja Balle, Thomas Drake, and Tom Dieth. 2020. Privacy- and Utility-Preserving Textual Analysis via Calibrated Multivariate Perturbations. In *WSDM '20: The Thirteenth ACM International Conference on Web Search and Data Mining, Houston, TX, USA, February 3–7, 2020*, James Caverlee, Xia (Ben) Hu, Mounia Lalmas, and Wei Wang (Eds.). ACM, New York, NY, USA, 178–186. <https://doi.org/10.1145/3336191.3371856>
- [18] Team GLM, ;, Aohan Zeng, Bin Xu, Bowen Wang, Chenhui Zhang, Da Yin, Diego Rojas, Guanyu Feng, Hanlin Zhao, Hanyu Lai, Hao Yu, Hongning Wang, Jiadao Sun, Jiajie Zhang, Jiale Cheng, Jiayi Gui, Jie Tang, Jing Zhang, Juanzi Li, Lei Zhao, Lindong Wu, Lucen Zhong, Mingdao Liu, Minlie Huang, Peng Zhang, Qinkai Zheng, Rui Lu, Shuaiqi Duan, Shudan Zhang, Shulin Cao, Shuxun Yang, Weng Lam Tam, Wenyi Zhao, Xiao Liu, Xiao Xia, Xiaohan Zhang, Xiaotao Gu, Xin Lv, Xinghan Liu, Xinyi Liu, Xinyue Yang, Xixuan Song, Xunkai Zhang, Yifan An, Yifan Xu, Yilin Niu, Yuantao Yang, Yueyan Li, Yushi Bai, Yuxiao Dong, Zehan Qi, Zhaoyu Wang, Zhen Yang, Zhengxiao Du, Zhenyu Hou, and Zihan Wang. 2024. ChatGLM: A Family of Large Language Models from GLM-130B to GLM-4 All Tools. arXiv:2406.12793 [cs.CL] <https://arxiv.org/abs/2406.12793>
- [19] Otkrist Gupta and Ramesh Raskar. 2018. Distributed learning of deep neural network over multiple agents. *J. Netw. Comput. Appl.* 116 (2018), 1–8. <https://doi.org/10.1016/J.JNCA.2018.05.003>
- [20] Zecheng He, Tianwei Zhang, and Ruby B. Lee. 2019. Model inversion attacks against collaborative inference. In *Proceedings of the 35th Annual Computer Security Applications Conference, ACSAC 2019, San Juan, PR, USA, December 09–13, 2019*, David Balenson (Ed.). ACM, 148–162. <https://doi.org/10.1145/3359789.3359824>
- [21] Zecheng He, Tianwei Zhang, and Ruby B. Lee. 2019. Model inversion attacks against collaborative inference. In *Proceedings of the 35th Annual Computer Security Applications Conference, ACSAC 2019, San Juan, PR, USA, December 09–13, 2019*, David M. Balenson (Ed.). ACM, New York, NY, USA, 148–162. <https://doi.org/10.1145/3359789.3359824>

- [22] Zecheng He, Tianwei Zhang, and Ruby B Lee. 2020. Attacking and protecting data privacy in edge–cloud collaborative inference systems. *IEEE Internet of Things Journal* 8, 12 (2020), 9706–9716.
- [23] Matthew Honnibal and Ines Montani. 2017. spaCy 2: Natural language understanding with Bloom embeddings, convolutional neural networks and incremental parsing. (2017). To appear.
- [24] Prateek Jain, Purushottam Kar, et al. 2017. Non-convex optimization for machine learning. *Foundations and Trends® in Machine Learning* 10, 3-4 (2017), 142–363.
- [25] Joohyung Jeon and Joongheon Kim. 2020. Privacy-Sensitive Parallel Split Learning. In *2020 International Conference on Information Networking, ICOIN 2020, Barcelona, Spain, January 7-10, 2020*. IEEE, 7–9. <https://doi.org/10.1109/ICOIN48656.2020.9016486>
- [26] Ziang Li, Mengda Yang, Yaxin Liu, Juan Wang, Hongxin Hu, Wenzhe Yi, and Xiaoyang Xu. 2024. GAN You See Me? Enhanced Data Reconstruction Attacks against Split Inference. *Advances in Neural Information Processing Systems* 36 (2024).
- [27] Chin-Yew Lin. 2004. ROUGE: A Package for Automatic Evaluation of Summaries. In *Text Summarization Branches Out*. Association for Computational Linguistics, Barcelona, Spain, 74–81. <https://aclanthology.org/W04-1013>
- [28] Yinhan Liu, Myle Ott, Naman Goyal, Jingfei Du, Mandar Joshi, Danqi Chen, Omer Levy, Mike Lewis, Luke Zettlemoyer, and Veselin Stoyanov. 2019. RoBERTa: A Robustly Optimized BERT Pretraining Approach. *CoRR abs/1907.11692* (2019). [arXiv:1907.11692](http://arxiv.org/abs/1907.11692) <http://arxiv.org/abs/1907.11692>
- [29] Luca Melis, Congzheng Song, Emiliano De Cristofaro, and Vitaly Shmatikov. 2019. Exploiting Unintended Feature Leakage in Collaborative Learning. In *2019 IEEE Symposium on Security and Privacy, SP 2019, San Francisco, CA, USA, May 19-23, 2019*. IEEE, 691–706. <https://doi.org/10.1109/SP.2019.00029>
- [30] Stephen Merity, Caiming Xiong, James Bradbury, and Richard Socher. 2017. Pointer Sentinel Mixture Models. In *5th International Conference on Learning Representations, ICLR 2017, Toulon, France, April 24-26, 2017, Conference Track Proceedings*. OpenReview.net. <https://openreview.net/forum?id=Byj72udxe>
- [31] OpenAI. 2023. GPT-4 Technical Report. *CoRR abs/2303.08774* (2023). <https://doi.org/10.48550/ARXIV.2303.08774> [arXiv:2303.08774](https://doi.org/10.48550/ARXIV.2303.08774)
- [32] Dario Pasquini, Giuseppe Ateniese, and Massimo Bernaschi. 2021. Unleashing the Tiger: Inference Attacks on Split Learning. In *CCS '21: 2021 ACM SIGSAC Conference on Computer and Communications Security, Virtual Event, Republic of Korea, November 15 - 19, 2021*, Yongdae Kim, Jong Kim, Giovanni Vigna, and Elaine Shi (Eds.). ACM, 2113–2129. <https://doi.org/10.1145/3460120.3485259>
- [33] Andrew Paverd, Andrew Martin, and Ian Brown. 2014. Modelling and automatically analysing privacy properties for honest-but-curious adversaries. *Tech. Rep* (2014).
- [34] Xinchu Qiu, Ilias Leontiadis, Luca Melis, Alex Sablayrolles, and Pierre Stock. 2024. Evaluating Privacy Leakage in Split Learning. [arXiv:2305.12997](https://arxiv.org/abs/2305.12997) [cs.LG]
- [35] Alec Radford, Karthik Narasimhan, Tim Salimans, Ilya Sutskever, et al. [n. d.]. Improving language understanding by generative pre-training. ([n. d.]).
- [36] Alec Radford, Jeffrey Wu, Rewon Child, David Luan, Dario Amodei, Ilya Sutskever, et al. 2019. Language models are unsupervised multitask learners. *OpenAI blog* 1, 8 (2019), 9.
- [37] Colin Raffel, Noam Shazeer, Adam Roberts, Katherine Lee, Sharan Narang, Michael Matena, Yanqi Zhou, Wei Li, and Peter J. Liu. 2020. Exploring the Limits of Transfer Learning with a Unified Text-to-Text Transformer. *J. Mach. Learn. Res.* 21 (2020), 140:1–140:67. <http://jmlr.org/papers/v21/20-074.html>
- [38] Ahmed Salem, Yang Zhang, Mathias Humbert, Pascal Berrang, Mario Fritz, and Michael Backes. 2019. ML-Leaks: Model and Data Independent Membership Inference Attacks and Defenses on Machine Learning Models. In *26th Annual Network and Distributed System Security Symposium, NDSS 2019, San Diego, California, USA, February 24-27, 2019*. The Internet Society. <https://www.ndss-symposium.org/ndss-paper/ml-leaks-model-and-data-independent-membership-inference-attacks-and-defenses-on-machine-learning-models/>
- [39] Abigail See, Peter J. Liu, and Christopher D. Manning. 2017. Get To The Point: Summarization with Pointer-Generator Networks. In *Proceedings of the 55th Annual Meeting of the Association for Computational Linguistics (Volume 1: Long Papers)*. Association for Computational Linguistics, Vancouver, Canada, 1073–1083. <https://doi.org/10.18653/v1/P17-1099>
- [40] Xicong Shen, Yang Liu, Huiqi Liu, Jue Hong, Bing Duan, Zirui Huang, Yunlong Mao, Ye Wu, and Di Wu. 2023. A Split-and-Privatize Framework for Large Language Model Fine-Tuning. *CoRR abs/2312.15603* (2023). <https://doi.org/10.48550/ARXIV.2312.15603> [arXiv:2312.15603](https://doi.org/10.48550/ARXIV.2312.15603)
- [41] Reza Shokri, Marco Stronati, Congzheng Song, and Vitaly Shmatikov. 2017. Membership Inference Attacks Against Machine Learning Models. In *2017 IEEE Symposium on Security and Privacy, SP 2017, San Jose, CA, USA, May 22-26, 2017*. IEEE Computer Society, 3–18. <https://doi.org/10.1109/SP.2017.41>
- [42] Congzheng Song and Ananth Raghunathan. 2020. Information leakage in embedding models. In *Proceedings of the 2020 ACM SIGSAC conference on computer and communications security*. 377–390.
- [43] Chandra Thapa, Mahawaga Arachchige Pathum Chamikara, Seyit Camtepe, and Lichao Sun. 2022. SplitFed: When Federated Learning Meets Split Learning. In *Thirty-Sixth AAAI Conference on Artificial Intelligence, AAAI 2022, Thirty-Fourth Conference on Innovative Applications of Artificial Intelligence, IAAI 2022, The Twelveth Symposium on Educational Advances in Artificial Intelligence, EAAI 2022 Virtual Event, February 22 - March 1, 2022*. AAAI Press, 8485–8493. <https://doi.org/10.1609/AAAI.V36i8.20825>
- [44] Yuanyishu Tian, Yao Wan, Lingjuan Lyu, Dezhong Yao, Hai Jin, and Lichao Sun. 2022. FedBERT: When Federated Learning Meets Pre-training. *ACM Trans. Intell. Syst. Technol.* 13, 4 (2022), 66:1–66:26. <https://doi.org/10.1145/3510033>
- [45] Tom Titcombe, Adam J. Hall, Pavlos Papadopoulos, and Daniele Romanini. 2021. Practical Defences Against Model Inversion Attacks for Split Neural Networks. *CoRR abs/2104.05743* (2021). [arXiv:2104.05743](https://arxiv.org/abs/2104.05743) <https://arxiv.org/abs/2104.05743>
- [46] Hugo Touvron, Thibaut Lavril, Gautier Izacard, Xavier Martinet, Marie-Anne Lachaux, Timothée Lacroix, Baptiste Rozière, Naman Goyal, Eric Hambro, Faisal Azhar, Aurélien Rodriguez, Armand Joulin, Edouard Grave, and Guillaume Lample. 2023. LLaMA: Open and Efficient Foundation Language Models. *CoRR abs/2302.13971* (2023). <https://doi.org/10.48550/ARXIV.2302.13971> [arXiv:2302.13971](https://doi.org/10.48550/ARXIV.2302.13971)
- [47] Hugo Touvron, Louis Martin, Kevin Stone, Peter Albert, Amjad Almahairi, Yasmine Babaei, Nikolay Bashlykov, Soumya Batra, Prajwal Bhargava, Shruti Bhosale, et al. 2023. Llama 2: Open foundation and fine-tuned chat models. *arXiv preprint arXiv:2307.09288* (2023).
- [48] Valeria Turina, Zongshun Zhang, Flavio Esposito, and Ibrahim Matta. 2021. Federated or Split? A Performance and Privacy Analysis of Hybrid Split and Federated Learning Architectures. In *14th IEEE International Conference on Cloud Computing, CLOUD 2021, Chicago, IL, USA, September 5-10, 2021*, Claudio Agostino Ardagna, Carl K. Chang, Ernesto Damina, Rajiv Ranjan, Zhongjie Wang, Robert Ward, Jia Zhang, and Wensheng Zhang (Eds.). IEEE, 250–260. <https://doi.org/10.1109/CLOUD53861.2021.00038>
- [49] Praneeth Vepakomma, Otkrist Gupta, Tristan Swedish, and Ramesh Raskar. 2018. Split learning for health: Distributed deep learning without sharing raw patient data. *CoRR abs/1812.00564* (2018). [arXiv:1812.00564](https://arxiv.org/abs/1812.00564) [http://arxiv.org/abs/1812.00564](https://arxiv.org/abs/1812.00564)
- [50] Praneeth Vepakomma, Abhishek Singh, Otkrist Gupta, and Ramesh Raskar. 2020. NoPeek: Information leakage reduction to share activations in distributed deep learning. In *20th International Conference on Data Mining Workshops, ICDM Workshops 2020, Sorrento, Italy, November 17-20, 2020*, Giuseppe Di Fatta, Victor S. Sheng, Alfredo Cuzzocrea, Carlo Zaniolo, and Xindong Wu (Eds.). IEEE, 933–942. <https://doi.org/10.1109/ICDMW51313.2020.00134>
- [51] Yiming Wang, Yu Lin, Xiaodong Zeng, and Guannan Zhang. 2023. PrivateLoRA For Efficient Privacy Preserving LLM. *CoRR abs/2311.14030* (2023). <https://doi.org/10.48550/ARXIV.2311.14030> [arXiv:2311.14030](https://doi.org/10.48550/ARXIV.2311.14030)
- [52] Ronald J. Williams and David Zipser. 1989. A Learning Algorithm for Continually Running Fully Recurrent Neural Networks. *Neural Comput.* 1, 2 (1989), 270–280. <https://doi.org/10.1162/NECO.1989.1.2.270>
- [53] Maoqiang Wu, Guoliang Cheng, Dongdong Ye, Jiawen Kang, Rong Yu, Yuan Wu, and Miao Pan. 2024. Federated Split Learning With Data and Label Privacy Preservation in Vehicular Networks. *IEEE Trans. Veh. Technol.* 73, 1 (2024), 1223–1238. <https://doi.org/10.1109/TVT.2023.3304176>
- [54] Zongshun Zhang, Andrea Pinto, Valeria Turina, Flavio Esposito, and Ibrahim Matta. 2023. Privacy and Efficiency of Communications in Federated Split Learning. *IEEE Trans. Big Data* 9, 5 (2023), 1380–1391. <https://doi.org/10.1109/TBDDATA.2023.3280405>
- [55] Zongshun Zhang, Andrea Pinto, Valeria Turina, Flavio Esposito, and Ibrahim Matta. 2023. Privacy and efficiency of communications in federated split learning. *IEEE Transactions on Big Data* 9, 5 (2023), 1380–1391.
- [56] Lianmin Zheng, Wei-Lin Chiang, Ying Sheng, Siyuan Zhuang, Zhanghao Wu, Yonghao Zhuang, Zi Lin, Zhuohan Li, Dacheng Li, Eric P Xing, Hao Zhang, Joseph E. Gonzalez, and Ion Stoica. 2023. Judging LLM-as-a-judge with MT-Bench and Chatbot Arena. [arXiv:2306.05685](https://arxiv.org/abs/2306.05685) [cs.CL]
- [57] Ligeng Zhu, Zhijian Liu, and Song Han. 2019. Deep Leakage from Gradients. In *Advances in Neural Information Processing Systems*, H. Wallach, H. Larochelle, A. Beygelzimer, F. d'Alché-Buc, E. Fox, and R. Garnett (Eds.), Vol. 32. Curran Associates, Inc. [https://proceedings.neurips.cc/paper\\_files/paper/2019/file/60a6c4002cc7b29142def8871531281a-Paper.pdf](https://proceedings.neurips.cc/paper_files/paper/2019/file/60a6c4002cc7b29142def8871531281a-Paper.pdf)

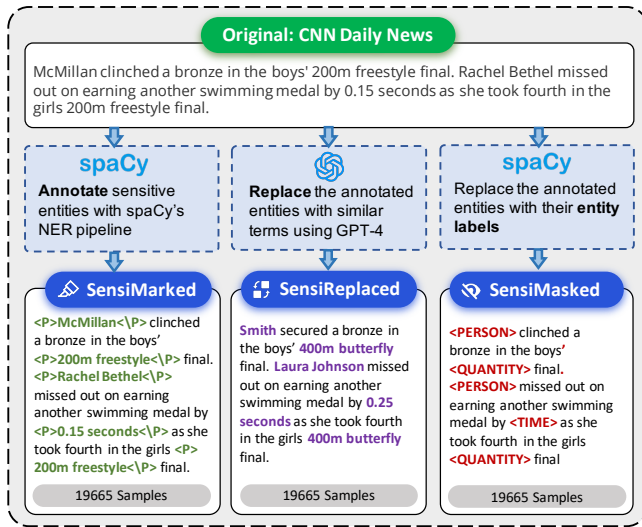


Figure 11: A detailed overview of the three Sensi-Series datasets derived from CNN DailyMail News, including processing methods and examples.

## A SPLIT LEARNING SIMULATION

In this work, the experiments for SL were conducted in a single-machine simulation environment. Using PyTorch and Huggingface Transformers APIs, we developed an easy-to-use SL simulation framework. By leveraging the equivalence between SL and centralized forward and backward propagation, the simulation was performed in a non-intrusive manner. Specifically, during training, we recorded the intermediate values of each block's forward propagation and the corresponding gradients without altering the model's forward and backward propagation processes.

We simulated the Client-Server architecture of SL systems in a serial manner. Specifically, we maintained the complete LLM in GPU memory while storing the parameters of different model segments (Bottom, Trunk, Top) from each client and the server in the main memory. In each round of SL, we loaded the Bottom and Top parameters of client1 and the Trunk parameters into the corresponding parts of the model in GPU memory. We then fine-tuned the LLM on the GPU using client1's data. After fine-tuning, we saved the Bottom, Top, and Trunk parameters back to the main memory. This process was repeated for client2 and subsequent clients. Once all clients had completed, we aggregated the Trunk parameters for that round. This serial simulation approach required hardware resources comparable to fine-tuning a single LLM on a single machine, allowing us to trade time for computational resources.

## B DATASET DETAIL

**B.0.1 Open-source Datasets.** To evaluate the overall attack performance of different DRA methods, we selected four commonly used open-source LLM instruction-tuning datasets to assess the data privacy vulnerabilities of LLMs during SFT under the SL framework. The datasets considered in the experiments include the natural language commonsense question-answering dataset

PIQA [5] (21k question-answer pairs), the encyclopedia text dataset WikiText2-v1 [30] (44.8k rows), the instructed code generation dataset CodeAlpaca-20K [8] (20k code generation instructions and corresponding code), and the math problem question-answering dataset GSM8K [11] (17.6k math problem question-answer pairs). Details of these datasets are provided in Table 8. Due to hardware limitations, all datasets were truncated to a maximum input length of 512.

**B.0.2 Customized Datasets: Sensi-Series.** To further investigate the attack performance of DRA methods on *sensitive information* and explore the attack mechanisms of learning-based approaches, we modified the open-source CNN-DailyMail News Text Summarization dataset [39] to manually construct a series of Sensitive datasets (hereafter referred to as *Sensi-Series*), as illustrated in Figure 11.

First, we created the *SensiMarked* dataset (19.7k rows) by annotating sensitive entities in the CNN-DailyMail News dataset using the NER pipeline of spaCy [23]. During testing on *SensiMarked*, we focused solely on the attack performance on these sensitive entities, thus eliminating the interference of frequently occurring common words on attack performance. The twelve types of sensitive entities are listed in Table 9. Next, leveraging these annotations, we used the GPT-4 API to randomly replace the pre-marked sensitive entities within the *SensiMarked* dataset, simulating a high-quality public dataset named *SensiReplaced* that attackers might obtain. The prompt template is as follows:

### Prompt Template of *SensiReplaced* Dataset

Replace given entities in the text with other random words.  
**Text:** [Text  $T$ ]  
**Given entities:** [Entities List  $\{E_i\}$ ]  
**Replaced text:**

Additionally, we anonymize sensitive entities in the *SensiMarked* dataset using labels corresponding to named entity types to create the *SensiMasked* dataset. The aim is to sanitize sensitive information within the dataset for further revealing the learning capabilities of attackers.

## C ATTACK EXAMPLES

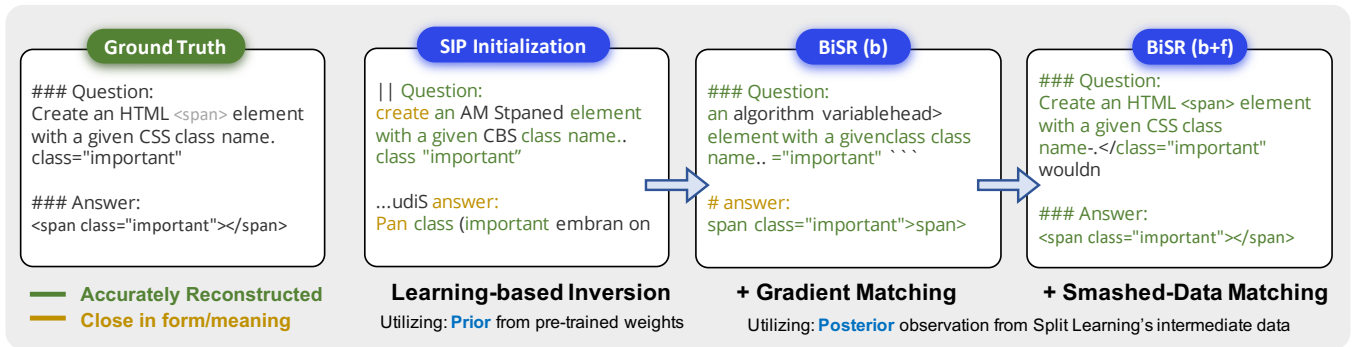
### C.1 Example of BiSR Attack

Figure 12 shows the multi-stage attack results of BiSR on a sample from CodeAlpaca. In this case, the SIP model was trained on *SensiReplaced*, a dataset that differs significantly from CodeAlpaca. As a result, while the initial attack by SIP successfully recovers a large number of tokens, it fails to accurately recover domain-specific tokens, such as code, due to this gap. This is where the optimization-based process of BRE comes into play, utilizing posterior information observed during SL (i.e., smashed data and gradients) to enhance the attack's accuracy. As shown in the figure, after gradient matching and smashed-data matching, the code tokens are successfully recovered. This demonstrates the significant advantage of BiSR in combining learning-based and optimization-based attack methods.



**Table 8: Details of the datasets used in our experiments.**

Dataset	# Samples	Task	Splits	Example
PIQA	21,035	Commonsense QA; Text classification	Train (77%) Test (14%) Validation (9%)	<b>Goal:</b> How to prevent pain while cutting your nails? <b>Sol1:</b> Dip your nails inside lukewarm water for 5 minutes before cutting. <b>Sol2:</b> Cutting nails doesn't cause pain as nails don't have sensation. <b>label:</b> 1
WikiText2-v1	44,836	Text Generation	Train (82%) Test (8%) Validation (10%)	<b>Text:</b> In the late 1920s, Barker began to doubt she was doing enough for the church and considered focusing solely on sacred works. Family and friends recommended she continue secular and sacred works, which she did. <b>Question:</b> James buys 5 packs of beef that are 4 pounds each. The price of beef is \$5.50 per pound. How much did he pay?
GSM8K	8,762	Math Problem QA	Train (85%) Validation (15%)	<b>Answer:</b> He bought $5 \times 4 = 20$ pounds of beef So he paid $20 \times 5.5 = \$110$ #### 110 <b>Prompt:</b> Create a SQL query to find the highest grossing movie. <b>Title Name:</b> "Movies" <b>Columns:</b> "MovieName", "Box-OfficeGross" <b>Completion:</b> SELECT MovieName FROM Movies ORDER BY BoxOfficeGross DESC LIMIT 1;
CodeAlpaca-20K	20,022	Instructed Code Generation	Train (90%) Validation (10%)	<b>Text:</b> <P>McMillan</P>clinched a bronze in the boys' <P>200m freestyle </P>final. <P>Rachel Bethel</P>missed out on earning another swimming medal by <P>0.15 seconds</P>as she took fourth in the girls <P>200m freestyle</P>final.
Sensi-Series	19,665	Text Generation	Train (60%) Test (25%) Validation (15%)	

**Figure 12: The outputs of BiSR's three-stage attack on a sample from CodeAlpaca. The portions of the sentence that were fully or nearly accurately recovered are highlighted in green and yellow, respectively.****Table 9: Named entity types of sensitive entities**

Type	Description
<PERSON>	People, including fictional
<GPE>	Countries, cities, states
<LOC>	Non-GPE locations
<DATE>	Absolute or relative dates or periods
<QUANTITY>	Measurements, as of weight or distance
<TIME>	Times smaller than a day
<PERCENT>	Percentage
<ORG>	Companies, agencies, institutions, etc.
<NORP>	Nationalities or religious
<MONEY>	Monetary values, including unit
<LAW>	Named documents made into laws
<WORK_OF_ART>	Titles of books, songs, etc.

## C.2 Example of NaMOE's Inversion Attack Under $d_{\chi P}$ perturbation

Figure 13 presents the attack results on a PIQA sample using the NaMoE model trained on SensiReplaced and a standard GRU model,

under different scales of  $d_{\chi P}$  perturbation applied to the target system. As shown, when the noise level is low ( $\epsilon' = 0.4$ ), both models can recover most of the information. However, as the noise level increases ( $\epsilon' = 0.1$ , where the model's fine-tuning loses utility), the GRU model struggles to recover any data, while NaMoE still manages to recover a substantial number of critical tokens. This demonstrates the effectiveness of noise-aware training in enhancing the noise resilience of inversion models.

## D DETAILED EXPERIMENT RESULT

### D.1 Attack Performance on Other metrics

In addition to ROUGE-L and METEOR, we assessed attack performance using two additional metrics: (1) ROUGE-1 [27], which measures the overlap of unigrams (single words) between the generated and reference texts, disregarding word order, and (2) Token Recovery Rate (TRR), which calculates the proportion of tokens in

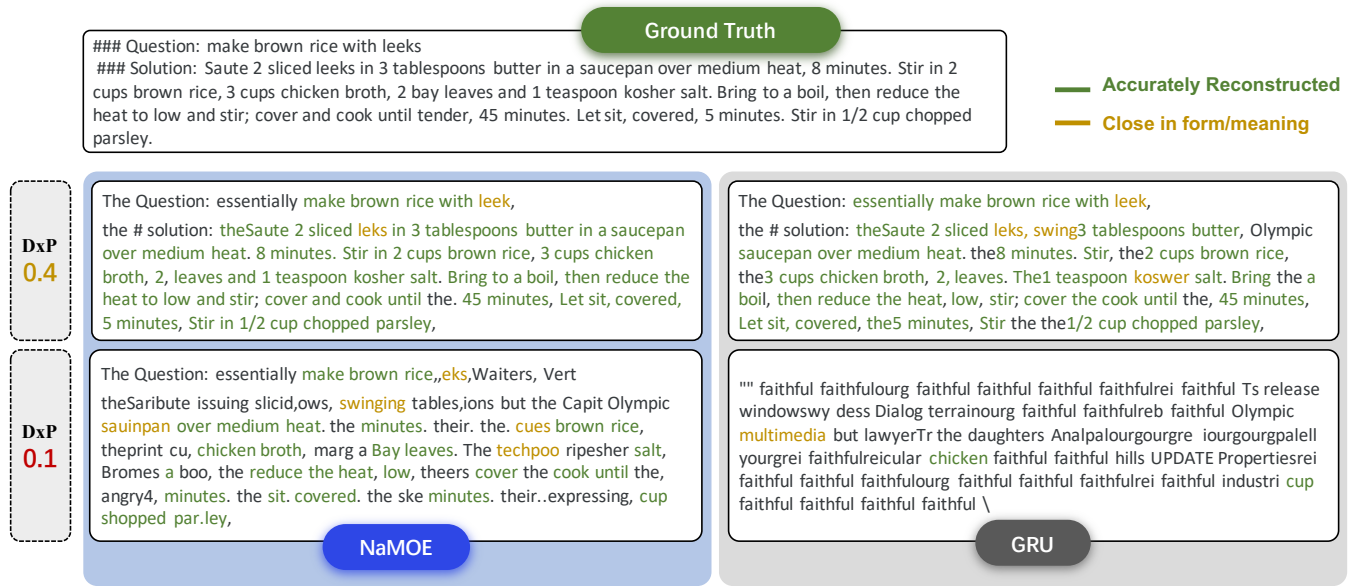


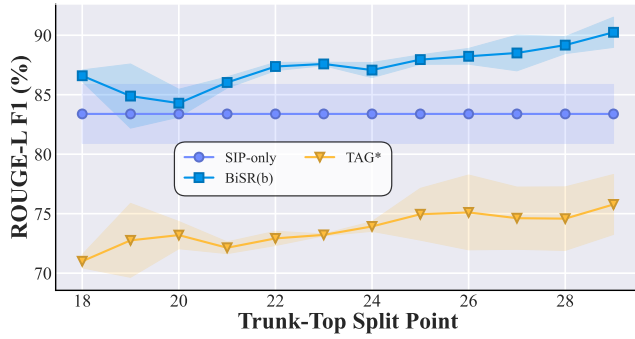
Figure 13: Comparison of attack results on a sample from PIQA between NaMoE and a standard GRU under varying levels of  $d\chi^P$  noise. The test LLM used is LLaMA2-chat-7B.

Table 10: Performance of BiSR (ROUGE-1 F1 % and Token Accuracy) on various LLMs fine-tuned on different datasets compared to alternative methods. Experiments utilized split points set at 6-26, with SensiReplaced serving as the auxiliary dataset  $D_a$ . The best results for each configuration are highlighted in bold, with the second best results underlined.

Model	Methods	Split Fine-tuning Datasets									
		SensiMkd		Codealpaca		Gsm8k		PIQA		WikiText	
		ROUGE-1-F	TokACC	ROUGE-1-F	Meteor	ROUGE-1-F	Meteor	ROUGE-1-F	Meteor	ROUGE-1-F	Meteor
LLa-MA2	AE	50.71±0.42	52.14±0.47	60.66±0.53	60.47±0.57	42.83±0.22	45.28±0.27	33.27±1.23	36.21±0.87	47.77±0.52	58.12±0.62
	EIA*	79.96±4.50	81.00±5.92	56.66±2.93	56.38±2.79	63.36±3.87	63.54±3.37	57.74±0.35	57.12±0.83	84.32±1.61	83.06±1.84
	TAG*	81.60±1.28	85.81±1.18	85.68±0.26	86.32±0.48	84.39±1.36	84.77±1.26	79.30±2.71	80.63±2.42	76.54±1.19	77.66±0.87
	LAMP*	80.83±0.48	84.40±0.21	84.39±0.29	85.21±0.31	84.85±0.33	85.03±0.39	77.67±0.99	78.86±0.98	76.33±0.86	77.33±0.81
	SIP-only	83.07±0.97	83.53±0.85	85.33±0.54	86.53±0.34	95.91±0.38	95.30±0.37	65.43±0.87	67.57±1.11	95.66±0.98	96.20±0.73
	BiSR(b)	90.33±1.81	90.94±1.60	90.82±0.70	90.40±0.80	96.40±0.36	95.68±0.39	83.24±1.14	82.73±1.29	96.80±0.78	97.49±0.66
	BiSR(f)	<u>92.87±1.95</u>	<u>90.46±1.85</u>	<u>95.33±0.17</u>	<u>93.35±0.28</u>	<u>98.12±0.36</u>	<u>97.17±0.48</u>	<u>88.24±1.52</u>	<u>85.08±1.45</u>	<u>98.70±0.58</u>	<u>98.69±0.44</u>
	BiSR	<b>95.62±0.23</b>	<b>92.28±0.28</b>	<b>95.99±0.18</b>	<b>93.53±0.07</b>	<b>98.48±0.25</b>	<b>97.57±0.42</b>	<b>92.72±0.69</b>	<b>88.50±0.77</b>	<b>99.64±0.26</b>	<b>99.43±0.32</b>
GPT2-large	AE	75.91±0.32	75.77±0.15	85.67±0.35	85.39±0.40	73.25±1.02	72.06±1.00	64.49±0.86	64.39±0.76	82.55±4.96	85.83±3.42
	EIA*	85.15±3.11	87.07±2.41	53.17±6.27	54.27±6.30	65.58±3.57	66.71±4.12	64.02±1.92	64.06±1.68	82.75±0.59	82.45±0.41
	TAG*	62.39±5.57	69.35±5.32	79.52±1.16	80.10±0.95	81.66±1.09	82.35±1.16	72.72±1.77	74.17±1.11	70.78±1.02	72.10±0.98
	LAMP*	60.51±0.31	69.91±0.61	78.65±0.16	79.02±0.20	78.29±0.53	78.17±0.11	70.16±0.36	71.40±0.13	70.49±0.14	71.87±0.14
	SIP-only	80.84±0.75	80.95±0.73	88.77±0.32	88.42±0.30	93.19±0.17	92.84±0.22	78.46±1.21	78.10±1.12	93.53±0.34	93.47±0.76
	BiSR(b)	88.33±0.69	87.77±0.73	94.87±0.31	94.60±0.30	95.80±0.18	95.74±0.26	91.23±0.31	90.74±0.29	97.28±0.75	96.80±0.28
	BiSR(f)	<u>95.07±0.60</u>	<u>94.46±0.94</u>	<u>97.22±0.81</u>	<b>96.75±0.90</b>	<u>99.06±0.29</u>	<u>99.07±0.34</u>	<u>92.36±1.15</u>	<u>90.84±1.47</u>	<u>99.71±0.26</u>	<u>99.56±0.51</u>
	BiSR	<b>95.20±0.83</b>	<b>94.47±0.98</b>	97.16±0.55	96.63±0.79	<b>99.14±0.11</b>	<b>99.17±0.13</b>	<b>92.64±0.70</b>	<b>91.23±0.98</b>	<b>99.79±0.29</b>	<b>99.62±0.54</b>
Chat-GLM3	AE	66.50±0.94	68.77±0.53	68.89±0.17	69.35±0.19	62.98±0.88	67.62±0.58	49.52±0.85	55.91±1.04	65.98±1.06	72.02±1.30
	EIA*	65.78±9.52	70.82±7.45	9.87±3.94	7.68±5.63	11.68±0.32	11.68±0.14	30.38±6.65	27.29±6.83	26.78±0.23	25.86±1.00
	TAG*	61.68±2.16	67.37±1.40	79.49±0.75	78.26±1.09	81.69±2.08	80.49±2.63	70.04±0.58	67.19±2.25	68.90±1.79	69.87±1.56
	LAMP*	39.21±0.13	50.50±0.18	78.25±0.39	77.58±0.46	79.48±0.32	79.58±0.35	70.31±0.34	66.97±0.10	69.03±0.52	69.62±0.52
	SIP-only	77.13±0.69	74.70±0.38	82.37±0.69	81.32±0.68	92.59±0.31	92.20±0.44	64.14±1.32	66.48±1.11	93.78±1.14	94.89±0.89
	BiSR(b)	<b>91.33±0.77</b>	<b>91.58±0.39</b>	<b>93.21±0.76</b>	<b>92.51±0.63</b>	<u>94.50±0.21</u>	<u>94.22±0.31</u>	<b>87.42±0.45</b>	<b>88.77±0.49</b>	94.96±1.29	95.85±0.76
	BiSR(f)	89.92±1.07	83.87±1.16	86.12±1.72	83.95±1.85	<b>99.72±0.10</b>	<b>99.54±0.15</b>	86.64±1.48	84.74±1.28	<u>100.00±0.00</u>	<u>100.00±0.00</u>
	BiSR	<u>90.90±0.31</u>	<u>90.08±0.52</u>	<u>86.54±1.96</u>	<u>85.38±2.12</u>	99.71±0.09	<u>99.53±0.17</u>	<u>86.68±1.52</u>	<u>85.57±1.27</u>	<b>100.00±0.00</b>	<b>100.00±0.00</b>

the reconstructed sentences that match those in the original sentences, also ignoring word order. Both metrics evaluate token-level reconstruction performance. The results for ROUGE-1 and TRR,

corresponding to Table 3, are presented in Table 10. These results reflect a consistent pattern with those in Table 3, demonstrating that DRAs can effectively reconstruct private information at both the token and sentence levels in the given setting.



**Figure 15: The impact of Trunk-Top split point on the attack performance of backward DRAs, tested on the LLaMA2-chat-7B and the PIQA dataset.**

**Table 11: Impact of LLM Quantization on BiSR’s Attack Performance (ROUGE-L F1 %  $\uparrow$ ) and LLM’s fine-tuning Performance (Perplexity on PIQA-test  $\downarrow$ ), tested on LLaMA2-chat-7B.**

Methods	Quantization								
	Raw			8-bit			4-bit		
	RgLF	Mtor	TRR	RgLF	Mtor	TRR	RgLF	Mtor	TRR
SIP	82.83	88.57	84.10	82.44	87.84	82.99	82.07	88.77	83.56
	$\pm 0.15$	$\pm 0.13$	$\pm 0.25$	$\pm 0.08$	$\pm 0.02$	$\pm 0.15$	$\pm 0.22$	$\pm 0.19$	$\pm 0.03$
BiSR(b)	89.66	93.68	90.64	89.46	93.58	90.15	86.85	91.50	87.08
	$\pm 0.27$	$\pm 0.27$	$\pm 0.03$	$\pm 0.99$	$\pm 1.21$	$\pm 1.03$	$\pm 0.47$	$\pm 0.06$	$\pm 0.31$
BiSR	95.97	97.97	92.29	95.54	97.51	92.12	96.80	98.65	93.20
	$\pm 0.09$	$\pm 0.03$	$\pm 0.43$	$\pm 0.20$	$\pm 0.17$	$\pm 0.29$	$\pm 0.37$	$\pm 0.05$	$\pm 0.15$
TestPPL	14.94 $\pm 0.04$			15.67 $\pm 0.01$			20.28 $\pm 0.14$		

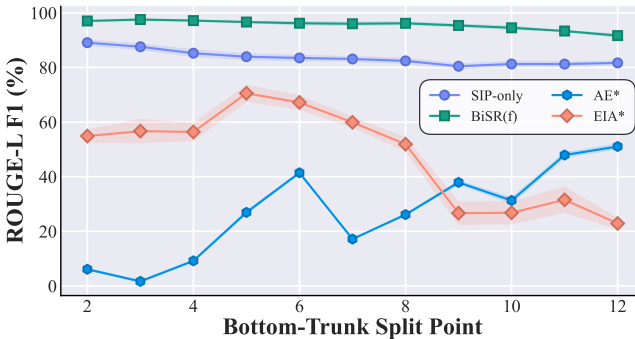


**Figure 14: The impact of Bottom-Trunk split point on the attack performance (ROUGE-L F1 Score %) of BiSR, in comparison with other forward DRAs, tested on the LLaMA2-chat-7B fine-tuned on the PIQA dataset.**

## D.2 NaMoE for NoPeek

For noise-aware training of the NaMoE model, we employed a *simulated fine-tuning* strategy. To produce NoPeek-perturbed intermediate results with parameter  $\alpha$ , we first fine-tuned the LLM on SensiReplaced using NoPeek noise with  $\alpha$  (600 steps in our experiment). The fine-tuned LLM then generated the intermediate results for NaMoE training. Given the high cost of fine-tuning, this strategy also required modifying the random noise approach during

NaMoE’s gating training phase. Consequently, we pre-fine-tuned 20 LLM models (LoRA adapters) with random-scaled NoPeek perturbations for NaMoE’s gating training. During each gating training step, one of these 20 models was selected to generate the simulated random-scaled NoPeek-perturbed smashed data.

## D.3 Impact of Split Points

**D.3.1 Bottom-Trunk Split Point.** The choice of split point in the Bottom-Trunk interface significantly impacts the performance of DRAs based on smashed data (forward DRAs), as intermediate representations that are farther from the input may contain less information about the original input, and a larger Bottom can increase the difficulty of search-based attacks. We tested the effects of different shallow split points on the performance of forward DRAs using the LLaMA2-7B-chat model and the PIQA dataset. These DRAs include the learning-based SIP and AE, as well as the optimization-based EIA and BiSR(f). As shown in Figure 14, deeper split points significantly degrade the performance of the optimization-based method EIA\*, with its effectiveness dropping from over 60 to 20. While BiSR(f) also experiences a slight performance decline at deeper split points, it still outperforms SIP, demonstrating that forward optimization can still offer advantages. The learning-based SIP also shows a similar, slight decline in performance. Interestingly, AE’s performance improves as the depth increases.

**D.3.2 Trunk-Top Split Point.** Similarly, the number of model layers in the Top part affects the performance of backward DRAs, i.e., gradient-matching-based attacks represented by TAG and BiSR(b). Therefore, we observed the impact of different Trunk-Top split points on attack performance (for example, for LLaMA2-7B with 32 blocks, a Trunk-Top split point of 28 means the last five decoder blocks are treated as the Top segment), as shown in Figure 15. Overall, the fewer the number of Top layers, the higher the performance of the gradient attack.

## D.4 Impact of Quantization

In practical LLM fine-tuning scenarios, quantization is a commonly used technique. Quantizing LLMs to lower precision types significantly reduces memory usage and accelerates computation time. In our experiments, due to resource limitations, we used 8-bit quantized versions for billion-parameter LLMs by default. To investigate the impact of quantization on BiSR in more detail, we fine-tuned different quantized versions (8-bit and 4-bit) of LLaMA2-chat-7B on PIQA, measuring fine-tuning performance using Test-Perplexity (TestPPL) and conducting attacks. As shown in Table 11, although LLM performance decreases with higher quantization levels (indicated by increased perplexity), quantization does not significantly affect the attack performance of BiSR.

## D.5 Impact of BRE’s Optimization Target

The forward optimization process in BRE, specifically smashed-data-matching, employs a continuous optimization strategy in the embedding space (rather than in the discrete vocabulary space). Beyond hyperparameters, the choice of the objective function is also critical. We compared two loss functions—Euclidean distance (L2-Norm) and cosine similarity—during the forward attack (BiSR(f)) on LLaMA2-chat-7B. As shown in Figure 16, “Normal” refers to

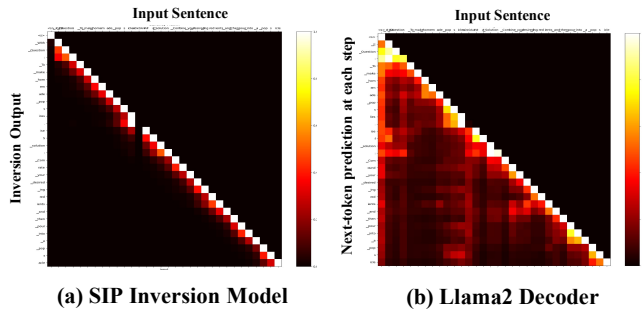


Figure 17: Heatmaps for an example from PIQA showing the contribution of each token position in the intermediate outputs of LLaMA2-chat-7B’s 6th layer to each position of the model output: (a) the reconstructed sentence by the inversion model, and (b) LLaMA2’s next-token prediction at each position. These heatmaps illustrate the model’s attention during inference.

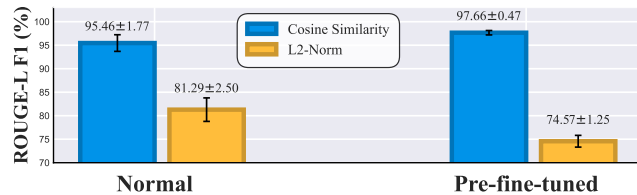


Figure 16: Comparison of the attack performance (ROUGE-L F1 Score%) and sensitivity to model parameter changes for the two objective functions used in smashed data matching in BRE. “Normal” refers to attacking a pre-trained LLaMA2 model, while “Pre-fine-tuned” refers to attacking a LLaMA2 model fine-tuned on CodeAlpaca.

Table 12: Attack performance (ROUGE-L F1%, Meteor%, TokACC) of different inversion models (trained on SensiReplaced) on LLaMA2-chat-7B (attack on the 6-th layer) and PIQA dataset.

	Linear	LSTM	SelfAttn	GRU(bi)	GRU
RougeLF	77.15±0.93	80.72±0.64	76.32±1.53	82.91±0.72	<b>83.54±1.16</b>
Meteor	86.88±0.27	86.76±0.20	85.46±1.41	88.03±0.18	<b>88.58±0.69</b>
TokACC	77.69±0.72	80.92±0.65	76.83±1.62	83.21±0.55	<b>83.92±0.78</b>

directly attacking an SL system fine-tuned on PIQA, while “Pre-fine-tuned” refers to attacking a system with parameters slightly deviated from the pre-trained state (i.e., pre-fine-tuned on CodeAlpaca). The results indicate that cosine similarity significantly outperforms L2-Norm, achieving better performance and greater robustness to parameter changes. In contrast, L2-Norm exhibits performance degradation as the model parameters vary, likely due to cosine similarity’s superior handling of the curse of dimensionality.

## E A MORE DETAILED INSPECTION OF SIP INVERSION MODEL

We have conducted extensive experiments demonstrating the strong recovery performance of SIP across different intermediate layers

of various model architectures. However, this leads to a curious question: *How much of the original input information is actually retained in the intermediate outputs of LLM? And on what basis does the SIP model perform its recovery?* To explore these questions, we conducted a series of observational experiments.

### E.1 Comparison of Different Inversion Models

We explored several commonly used models for the structure of SIP, including a simple linear model (Linear), LSTM, a single Self-Attention layer (SelfAttn), GRU, and a bidirectional GRU model (GRU(bi)). We compared their performance in inversion attacks on the output of the 6th layer of LLaMA2-chat-7B using the PIQA dataset. As shown in Table 12, even the simple linear model achieves notably high attack performance, highlighting the significant privacy information contained in the intermediate results. The unidirectional GRU achieved the best attack performance, making it the default SIP model in our experiments and a component of NaMoE.

### E.2 Visualization of SIP Inversion Attack

To further investigate the GRU model’s recovery behavior on LLM intermediate outputs, we employed gradient-based feature attribution methods. We generated heatmaps comparing the GRU model’s output relative to its input smashed data with the LLM’s decoder output (next-token prediction at each step) relative to the same smashed data, as shown in Figure 17. It is evident that the unidirectional GRU’s “preceding sequence-only” focus aligns with the attention mechanism of causal language models. However, during text reconstruction, the GRU focuses on the current token and the preceding few token positions, demonstrating a much narrower attention span compared to LLMs. The GRU’s ability to achieve high reconstruction performance despite its narrower focus suggests that it performs inversion primarily based on the intermediate representation of individual tokens rather than on the interaction between different tokens’ intermediate representations. This also indicates that the high-dimensional intermediate representations (hidden states) of LLMs contain rich information about the raw input tokens. This observation aligns with the hypothesis drawn from the mutual attack experiments on the Sensi-Series Datasets discussed in Section 4.2.

### E.3 Impact of LLM’s Hidden Dimensionality

The hypothesis that the high-dimensional intermediate representations of tokens support SIP reconstruction attacks prompted us to investigate: *What is the minimum dimensionality of intermediate representations that can sustain high-performance SIP attacks?* To explore this, we conducted experiments on LLaMA2-chat-7B, focusing on hidden dimensionality. Specifically, we progressively reduced the intermediate dimensions of the LLM and observed the changes in attack performance (measured by ROUGE-L % ↑ on PIQA) and the LLM’s own performance (measured by Testing Perplexity ↓ on PIQA). Assuming the original hidden dimensionality of the LLM is  $D$ , we simulated reduced intermediate dimensions by training a pair of dimensionality reduction-expansion matrices,  $A^{D \times \alpha}$  and  $B^{\alpha \times D}$ . The output  $h$  of a specific layer (in this case, the 6th layer) is first processed by these matrices, resulting in  $hAB$ ,

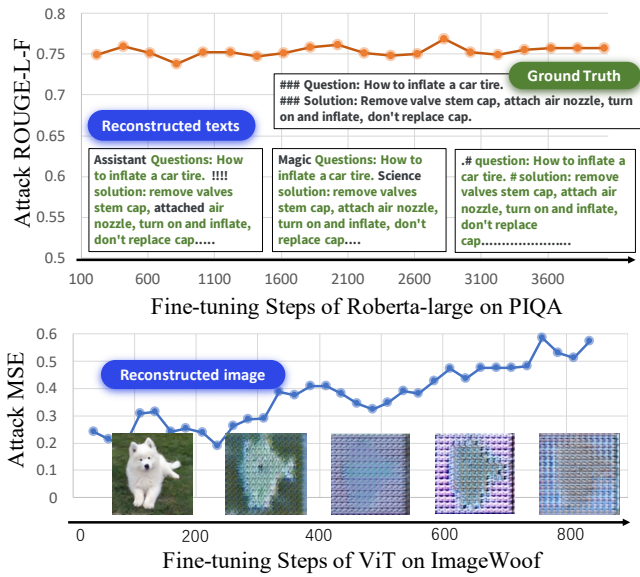


**Figure 19:** A comparison of the attack performance on language models (Top) and image models (Bottom) as the number of fine-tuning steps on the target model changes. For language models, the attack targets the sixth layer output of the Roberta-large model, fine-tuned for a binary classification task on the PIQA dataset, with attack performance evaluated using RougeL-F1 (higher is better). For image models, the attack targets the sixth layer output of the ViT-large model, fine-tuned for a multi-classification task on the ImageWoof dataset, with attack performance evaluated using MSE (lower is better).

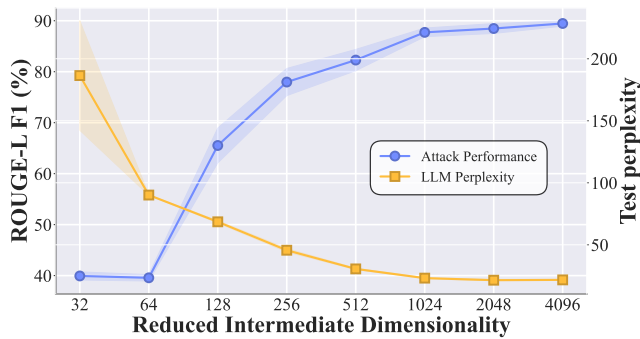


**Figure 18:** The impact of intermediate representation dimensionality (simulated via dimensionality reduction) in LLM (LLaMA2-chat-7B) on its own performance (test perplexity ↓ on PIQA) and the attack performance (ROUGE-L F1 Score %) of an SIP model trained on SensiReplaced.

which is then fed into the next layer. We pre-trained these matrices on SensiReplaced to ensure that their output mirrors the input as closely as possible. We then applied a pre-trained  $AB$  to the target LLM, allowing the SIP inversion model to attack the intermediate output  $h_p^{S \times D}$  of a sensitive sample after dimensionality reduction, resulting in  $(h_p A)^{S \times \alpha}$ .

As shown in Figure 18, both model performance and attack performance improve as the intermediate dimensionality  $\alpha$  increases. However, even with an intermediate dimensionality of just 32, SIP is still able to recover 40% of the data, with the increase in attack performance significantly outpacing the improvement in model performance. For example, when  $\alpha$  reaches 128, the attack performance sharply increases to over 60%, while the model’s performance sees only a modest gain. This suggests that while the intermediate representations of LLMs are low-rank, the information related to the original input tokens is more easily retained in low-rank representations compared to the information needed to support language modeling.

## F COMPARISON WITH VISION MODELS

To investigate whether Assumption 1 holds for other models following the pretrain and fine-tune paradigm, we adapted the SIP attack method to the Transformer-based vision model ViT [14]. For ViT’s intermediate outputs, we first captured their sequence information using a unidirectional GRU, followed by reconstructing the images through multiple deconvolution layers. Using MSE as the loss function, we trained this model on the 6th layer output of a pretrained ViT-large using the ImageWoof test set. The model successfully converged on the training dataset and exhibited good recovery performance on the test set. We then applied it to attack a ViT model undergoing split fine-tuning on the ImageWoof train set for a multi-classification downstream task. However, unlike text models, as fine-tuning of the target system progressed, the performance of the attack model trained in this manner significantly deteriorated, as shown in Figure 19.

In contrast, an attack on the language model Roberta, performing a text classification task with a similar parameter scale, demonstrated robustness against the target system’s fine-tuning, as depicted in Figure 19. After two epochs of fine-tuning on PIQA, the attack model’s performance was not notably affected. Based on this observation, we preliminarily conclude that semi-white-box settings pose a greater privacy risk in the context of language models, as the features of intermediate outputs learned by learning-based methods may not change significantly with LLM fine-tuning on downstream tasks. In other words, Assumption 1, i.e., Not-too-far, holds true. In contrast, for image models, a semi-white-box setting leans more towards a black-box scenario, indicating that the effectiveness of attacks using pre-trained parameters is more limited.